Landslides (2020) 17:1063–1081
DOI 10.1007/s10346-019-01338-w
Received: 1 August 2019
Accepted: 18 December 2019
Published online: 10 January 2020
© Springer-Verlag GmbH Germany
part of Springer Nature 2020

G. Pappalardo · S. Mineo · S. Imposa · S. Grassi · A. Leotta · F. La Rosa · D. Salerno

A quick combined approach for the characterization of a cliff during a post-rockfall emergency

Abstract The research presented in this paper is aimed at testing an innovative surveying protocol based the integration of quick methodologies employed for the characterization of a carbonate cliff affected by a rockfall and showing signs of further instability. During a post-rockfall emergency, one of the most important activities is evaluating if reactivation of the movements is possible, and if it may represent a threat for a series of elements at risk. On 5 January 2019, intense rainfalls triggered the detachment of a significant volume of fractured limestone and dolostone below the main square of a historical village located in southern Italy in the municipality of Messina, giving rise to one of the greatest landslides occurred at one of the most tourist areas of northeastern Sicily. Fallen blocks damaged the two main infrastructures of the area reaching also a bus terminal, which fortunately was vacant at the time of the rockfall. With the aim of proposing a quick surveying protocol during a post-rockfall emergency, terrestrial laser scanner, infrared thermography, and horizontal to vertical spectral ratio surveys were employed for the geostructural characterization of the cliff and for the investigation of the subsoil below the main square. In particular, the survey through terrestrial laser scanner returned an accurate 3D model of the cliff, where some key structures were highlighted; infrared thermography allowed recognizing caves and fractures along the cliff, with specific reference to a hollow area arising from past rockfalls. Such remote data, along with direct rock mass surveys performed by expert climbers allowed ascertaining that the instability of this cliff is driven by wedges formed by the intersection of 2 and 3 discontinuity systems, which are likely related to the main tectonic systems of the area. The horizontal to vertical spectral ratio survey allowed the identification of a peculiar vertical contrast of impedance, which may be related to a mechanical discontinuity located below the main square of the village, well matching with one of the systems responsible of the instability. The integration of these surveys methodologies resulted a useful quick protocol for the achievement of the key information on the stability of a rock cliff in the initial stage of its securing.

Keywords Rock cliff · Rockfall · Infrared thermography · Laser scanner · HVSR

Introduction

In a post-rockfall emergency, the quick survey of affected areas is essential to ensure a rapid characterization of the problem, forecast its potential evolution and suggest the most suitable urgent remedial measures. To this purpose, the integration of quick survey methodologies is welcomed for the management of the emergency, especially when no previous engineering-geological data are available and the most exposed elements at risk have to be located. When the setting of rock cliffs does not offer suitable spots for direct rock mass surveys or the unstable rock volumes are located at relevant heights, the remote and/or indirect analysis of the main geostructural features is a feasible solution to achieve reliable data.

The recent technological development in the analysis of slope instability has highlighted the potential of some innovative, non-destructive, and stand-alone survey methodologies acting from both a remote position (e.g., terrestrial laser scanner, infrared thermography) and in situ (geophysical HVSR prospecting). More specifically, terrestrial laser scanner (TLS) provides detailed point cloud data to obtain a highly accurate 3D model of the slope, thus overcoming the limitations of traditional surveying methodologies applied to high cliffs or to hardly accessible rock faces, although a direct rock mass survey, when feasible, is welcomed for a more realistic interpretation of TLS results. The scientific literature offers numerous cases of TLS application for the study and monitoring of rock masses (e.g., Lim et al. 2005; Rosser et al. 2005; Armesto et al. 2009; Fanti et al. 2012; Abellán et al. 2013; Gigli et al. 2014a; Mineo et al. 2018). Its most significant advantage is the possibility of achieving the accuracy of the best topographic instruments, thus ensuring a precise analysis of the rock face, with the possibility of focusing on the main instability features.

Infrared thermography (IRT) is a particular imaging technique based on the infrared radiation emitted by all forms of matter with temperature above the absolute zero (Hillel 1998). Its application to the rock mechanics as a diagnostic tool for instability phenomena has still a limited case history. It allows building images highlighting the thermal variations occurring along a rock slopes, which can be related to specific features of the rock. The most recent experiences proved the usefulness of IRT for either the study of weathered unstable slopes, or the rock mass fracturing characterization, or the remote survey and mapping of large landslides (Baroň et al. 2012; Casagli et al. 2017; Pappalardo et al. 2018a; Pappalardo and Mineo 2019). Some application cases in literature are focused on the integration between IRT and geomechanical surveys and/or TLS (e.g., Gigli et al. 2014b; Martino and Mazzanti 2014; Mineo et al. 2015a, b; Teza et al. 2015; Pappalardo et al. 2016a).

The horizontal to vertical spectral ratio (HVSR) is an indirect geophysical surveying methodology employed for the calculation of the spectral ratio between the mean horizontal on the vertical components of the ground motion (Nakamura 1989). HVSR technique allows identifying the amplification frequency of the ground motion due to resonance effects. This can be related to the presence of tectonic and/or stratigraphic discontinuities, landslides, or peculiar local conditions. Several authors employed HVSR technique to get information on the seismostratigraphy features of the subsoil (e.g., Lermo and Chavez-Garcia 1993; Lachet and Bard 1994; Ibs-von Seht and Wohlenberg 1999). Pappalardo et al. (2016b) coupled this survey method to geostructural analyses to reconstruct the degree of fracturing of a rock cliff in a cultural heritage site previously investigated from the geostructural point of view (Imposa et al. 2010, 2015), while Imposa et al. (2017a) proved its utility in the survey of a landslide body. A successful application was achieved also by Pappalardo et al. (2018b), who detected a relict landslide underneath an archeological site in Sicily.

Although these surveying techniques provide different outputs, their coupling for the investigation of a stability problem gains a scientific interest in the perspective of an emergency surveying procedure.

In this frame, the abovementioned methodologies have been herein combined for the analysis of a rock cliff in northeastern Sicily affected by a rockfall, which occurred in January 2019 at Castelmola, counted among the most "beautiful villages of Italy" (Bacilieri 2019) (Fig. 1a). It involved about 20 m^3 of rocks, which fell in a high-risk area (Mineo et al. 2017) causing damages and the temporary closure of the only access road, leading to the isolation of the place and the need of urgent remedial works. The predisposition to rockfall of this area is due to the peculiar geological and tectonic and features, with intensely fractured carbonate rock lithologies overlapping a weathered, low-grade metamorphic basement.

The scientific purpose of this research is therefore to test the potential of a quick integrated survey protocol, which allowed facing the problem from two sides. From one, TLS and a rock mass survey performed by expert climbers provided a 3D reconstruction of the geometry of the slope to gain the main geostructural model on the rock face highlighting the main criticalities. IRT returned hints on the condition of the rock at the top of the cliff, providing a better definition of the main geostructural features and identifying potential forthcoming rockfalls, along with some key discontinuity systems and the presence of water circulation. On the other hand, a geophysical HVSR-MASW survey was carried out on the top of the cliff, where the main square of the village lays. In fact, the source area of the 2019 rockfall is located below the square pavement. Therefore, the investigation on the integrity of the rock mass at this spot is essential in the perspective of potential retreat phenomena, which would threat the stability of the village itself. All the surveys were performed in 2 working days, to ensure the rapidity of work, which is fundamental in the management of an emergency state.

The study area: geology and rockfalls over the years

Main geological and geostructural outlines

The study area is located on the Peloritani Mountains, which can be defined as a nappe-pile edifice made of different tectonic slices of metamorphic basement and Mesozoic–Cenozoic sedimentary covers (Lentini et al. 2006). Crystalline Hercynian formations are overlapped by sedimentary series spanning from Early Lias to Olocene. Outcrops are displaced by regional fault systems, oriented W–E, NW–SE, and NNW–SSE, which are counted among the main cause of the frequent seismic activity of this regional sector (Tortorici et al. 1985). This is a significant aspect, as the seismicity is one of the triggering causes of rockfalls (e.g., Marinos and Tsiambaos 2002; Barbano et al. 2014).

Castelmola village lies on the top of a carbonate cliff, whose rocks belong to the Longi Taormina Unit, represented by lower Liassic grayish-white limestones and dolostones in carbonate platform facies (Lentini et al. 2006) (Fig. 1b). Such lithology unconformably lies on Triassic fluvial "Verrucano-type" deposits, in turn overlapping the crystalline basement.

The geostructural setting of the rock masses cropping out in the area has already been studied for several purposes in the latest years (e.g., Ferrara and Pappalardo 2005; Pappalardo et al. 2014; Pappalardo and Mineo 2015). Rock masses are made of carbonate rocks of Triassic age, ranging from limestones to dolostones, with intraformational transitions. Rocks belonging to this formation are characterized by a high degree of fracturing and variable mechanical behavior (e.g., Pappalardo 2015; Pappalardo and Mineo 2016). Rock masses are affected by numerous discontinuity systems, which cause a reduction of the unitary rock volume of the rock in some portions of the outcrops and show a poor to fair geomechanical quality according to Bieniawski (1989).

Past rockfalls: state of the art

The study area has been suffering consequences arising from rockfall events for decades. Blocks usually detach from the higher sectors of the Castelmola cliff affecting private and public structures. The main strategic element at risk is the Provincial Road 10 (SP-10), which is the only access road to the village traveled also by thousands of tourists every year due to the cultural heritage relevance of this site (Fig. 2a). Most of the ancient landslide events, especially those which did not affected structures/road or involved small rock volumes, were not documented or reported to the local authorities, while some of the most relevant ones are collected in national catalogs such as the AVI project (Italian Areas of Vulnerability; AVI Project 1998) and P.A.I. (Piano stralcio per l'Assetto Idrogeologico 2006). Pappalardo et al. (2014) and Pappalardo and Mineo (2015) presented a chronological reconstruction of the main rockfalls starting from 1952, when a landslide affected the only access way to Castelmola after heavy rainfalls. Similar events cause the temporary road disruption, leading to severe damages for the local economy and representing an obstruction if an evacuation is needed. In the 1990's, three main events led to the SP-10 disruption, with significant rock volumes detached by the highest cliff portions (Ferrara and Pappalardo 2005). In particular, the 1999 rockfall involved a car causing no injuries. In 2006, the fall of a 6-m^3 boulder close to a private house complex prompted the construction of a rockfall barrier aimed at protecting this local settlement standing at the foot of the cliff (Fig. 2b). In February 2012, two different blocks reached the SP-10 bringing damages to some elements of the carriageway. These are only the documented events available in the local chronicle reports and in literature, but the presence of widespread blocks along the slopes and along the SP-10 carriageway suggests how frequently rockfalls occur in this area. With the aim of providing a risk zonation at the threatened strategic access road, Pappalardo et al. (2014) and Mineo et al. (2017) highlighted the high rockfall risk affecting such transportation corridor and the most critical sector deserving in-depth studies. Their outcomes arise from the study of the most recent events occurred in August 2013 and February 2015. The first one involved three blocks, which reached both the previously mentioned house complex and the downstream road after having bypassed the rockfall barrier (Fig. 2c, d). The peculiarity of this event is that one of the three blocks reached the SP-10 road exactly at a parking area employed as a bus terminal, without causing injuries. In 2015, two further blocks detached northward and stopped on the roadside, leading to a temporary disruption of the SP-10 (Fig. 2).

On 16 November 2016, heavy rainfalls triggered the detachment of a great volume of rock mass, which impacted at the foot of the vertical cliff breaking up into smaller volumes. Four of these (with

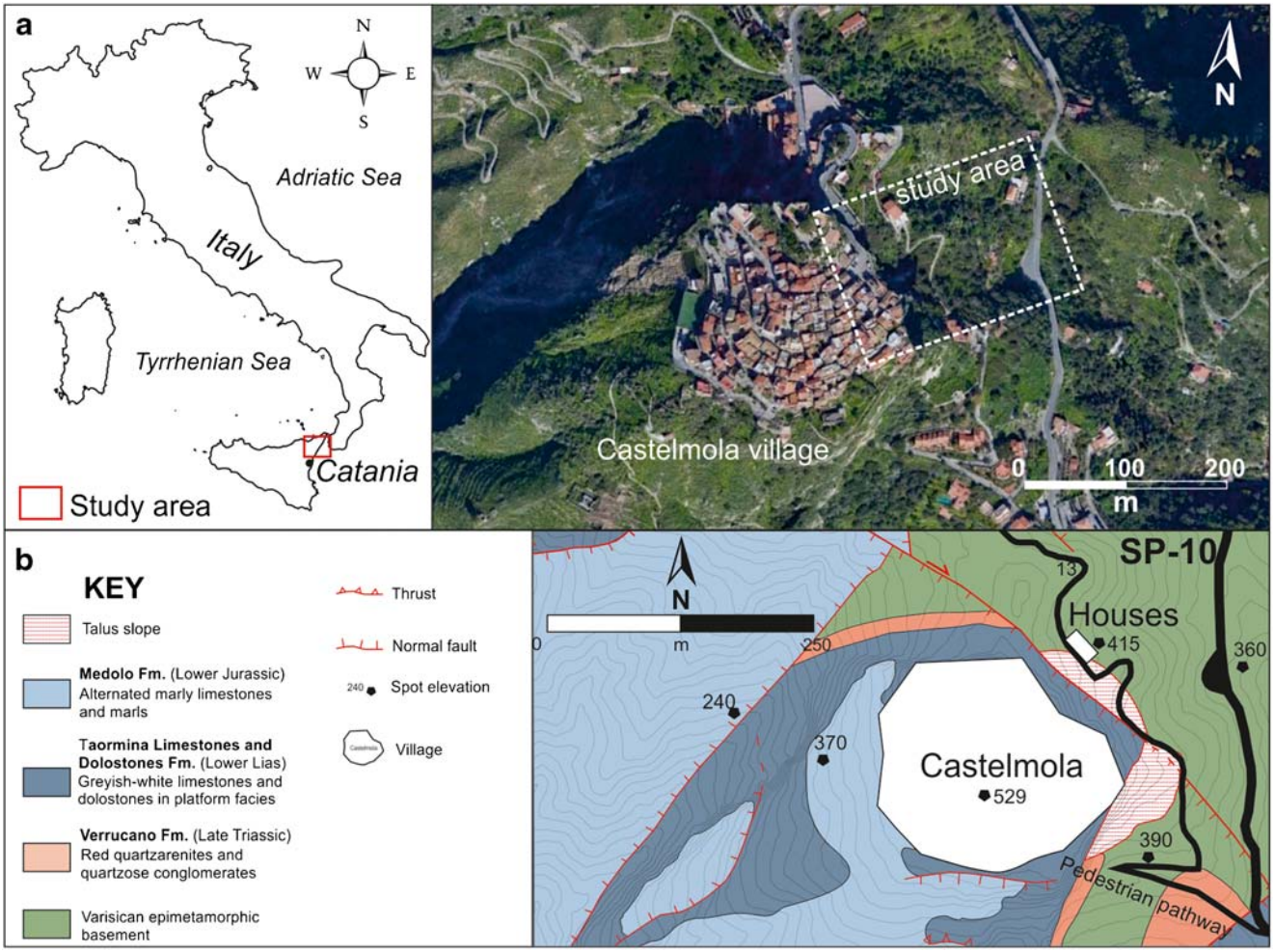

Fig. 1 **a** Geographical location and **b** geological map of the study area

volumes ranging from 0.5 to > 1 m^3) reached the access path to the house complex after having rolled for about 50 m. In this case, such pedestrian path (PP) acted as a catchment area for the boulders, which did not go on downstream, testifying how linear structures running at different altitude play a key role in a rockfall path (Mineo et al. 2017).

The 5 January 2019 rockfall

In the early afternoon of 5 January 2019, an intense rainfall event triggered the detachment of a significant volume of fractured limestone and dolostone, which slid along a dip-slope plane towards the impact point of the 2016 event (Fig. 3). This produced a 6 × 9 m large cavity under the main square of Castelmola village (detachment zone) famous for its panoramic view towards Taormina and the Ionian coastline, as the fallen rock mass was its hard basement. A comparison with an older photo of the cliff allows locating the detached rock volume, which showed signs of instability already in 2013 (Fig. 3). The rockfall was composed of about 25 main blocks (average volumes between 0.1 and 5 m^3) and numerous smaller rock volumes, which crossed the slope as far as the SP-10 road and the bus terminal already affected in 2014. In particular, three main runoff sectors can be identified: the first one is located right at the foot of the vertical cliff, where a change in the slope aspect characterizes the morphology. This is the point where the block movement turns from free-fall into rolling/rebounds. The greatest volumes proceeded downstream towards the other runoff sectors, i.e., the pedestrian pathway (PP) and the SP-10 (Fig. 3). The rockfall deposit shows a sort of gradation of volumes, with greatest blocks traveling a longer distance as far as the SP-10. In fact, 24 blocks stopped along a 30-m long segment of PP, damaging the road pavement and the railing. Their volume ranges from 0.1 to 2 m^3, and some of them show weathering films on the surface, index of water circulation on both the rock face and within open discontinuities. Traces of block transit towards downstream are evident in vegetated areas. Three main blocks reached the bus terminal and the SP-10, with volumes ranging between 1.3 and 5 m^3. Signs of their transit along the road are identified by impact craters on the asphalt (Fig. 3). Only 1 block invaded the SP-10, leading to its temporary disruption. Signs of weathering films on the block surface are present in some cases. An approximate estimation of the global mobilized volume, according to the size of the cavity left on the cliff, is about 60 m^3.

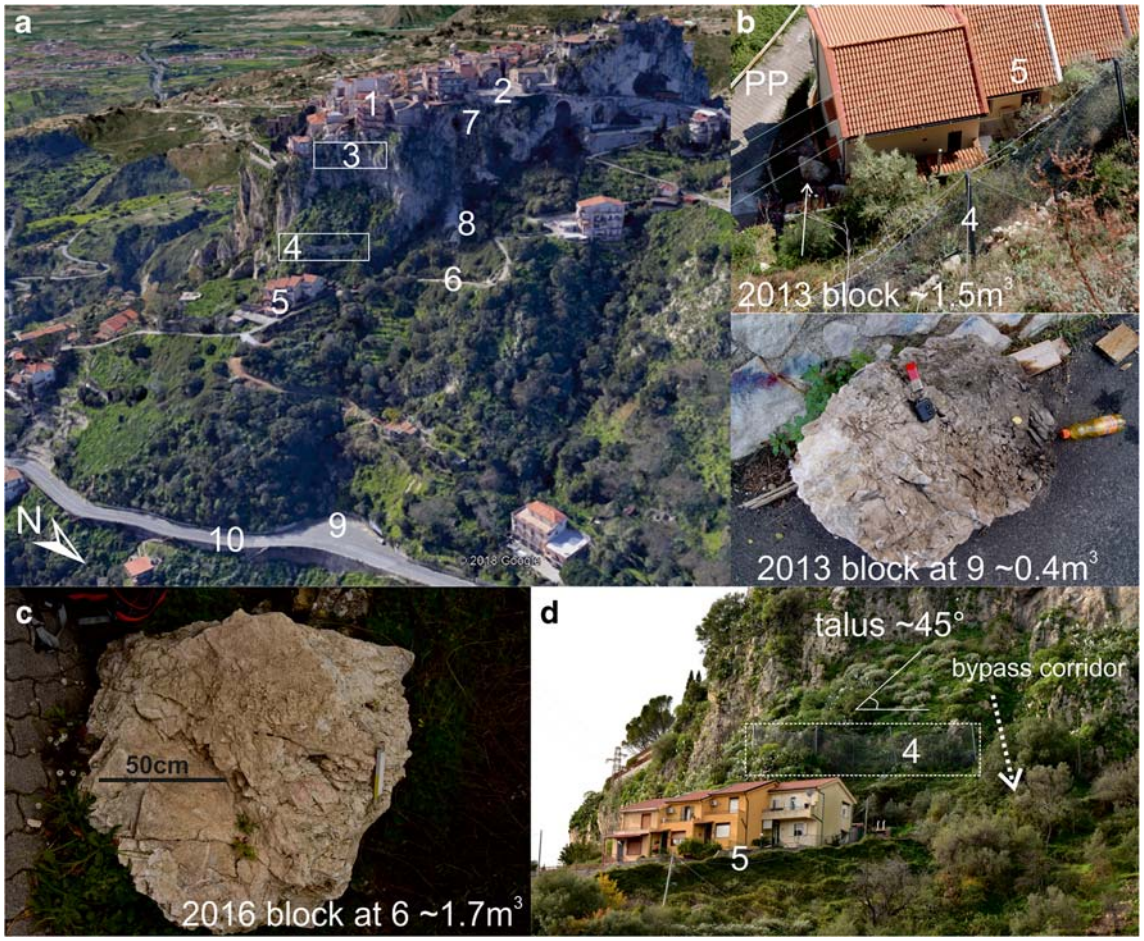

Fig. 2 **a** Panoramic 3D model of the Castelmola cliff (1 Castelmola village, 2 Main square, 3 2006 and 2013 source area, 4 rockfall barrier, 5 house complex, 6 pedestrian pathway PP, 7 2016 and 2019 source area, 8 2016 and 2019 talus, 9 bust terminal, 10 SP-10 road); **b** On of the blocks fallen in 2013; 2016 block at PP; view of the house complex and protecting rockfall barrier

A rockfall simulation was performed along this trajectory, based on the results of a back analysis, by the RocFall computer program (Rocscience) according to the "Lumped Mass" method and considering 10,000 possible trajectories of blocks with a reasonable volume for the 2019 event. This confirmed the presence of three main runoff sectors, located at (Fig. 4):

- the foot of the cliff, where about 50% of blocks stop;
- PP, where about 35% of blocks stop;
- SP-10, reached by about 3% of blocks.

The remaining rock volume stops along the vegetated slope. Although such percentages are affected by the limitation of the simulation method, which consider a constant mass of the boulder during the trajectory, this outcome proves that the studied rockfall is not a causality, but a potentially repetitive event representing a risk for the main infrastructures, as already pointed out by Mineo et al. (2017).

Methodological approach

The methodological approach followed herein (Fig. 5) is aimed at testing an innovative surveying protocol, based on the combination of different techniques, looking for a quick slope stability assessment, supported by the detection of the main criticalities in terms of potential reactivation of the movement. Indeed, this could lead to both cliff retreat phenomena (threatening the structures laying on its top) and to further damages to the elements at risk located at the foot of the slope, which in this case are represented by a group of houses and two linear infrastructures (a pedestrian tourist path and the only access road to the village).

In detail, a 3D model of the cliff was achieved by a TLS survey (Fig. 5), which allowed the reconstruction of a high definition point cloud for the generation of a mesh on which aerial photos, taken by an unmanned aerial vehicle, and IR images can be overlapped. In this perspective, IRT allows the remote mapping of the cliff face according to the detection of the surface temperature variations, which depend on peculiar feature of the slope (Fig. 5). In this way, the source area of the rockfall can be characterized locating cavities, open fractures, loose rock, presence of water, specific kinematic patterns. IRT allows indeed the detection of the most persistent cracks, highlighting their relationship in terms of identification of kinematic features, with specific reference to wedges. IRT outcomes were compared with the

Fig. 3 Reconstruction of the rockfall trajectory with a focus on the three key spots: 1, source area with a comparison between photos taken in 2013 and 2019; 2, surveyed blocks along PP; 3, surveyed blocks along SP-10

geostructural data collected on the rock face by expert climbers, and the thermograms were overlapped on the 3D model of the slope for a quicker interpretation of the data.

Moreover, in order to evaluate the degree of fracturing within the rock mass and to detect potential criticalities in the subsoil, HVSR surveys were performed on the main square at the top of

Fig. 4 2019 rockfall trajectory simulation with identification of the main runoff sectors

the cliff (Fig. 5). In this way, the amplification of the ground motion due to stratigraphic resonance, which returns information on the degree of fracturing of the rock mass, allowed highlighting the presence of key impedance contrasts related to particular discontinuities in the subsoil.

The integration of such survey methodologies represents an innovative approach for the analysis of unstable rock slopes and the management of rock fall risk, which can be taken into account for numerous similar cases worldwide.

Terrestrial laser scanner

TLS is a contact-free and ground-based technology for terrain and landscape high-resolution mapping, employed in several cases and integrated surveys (e.g., Teza et al. 2015; Martino and Mazzanti 2014). Such technology is based on the emission and subsequent reception of an electromagnetic pulse (laser). The time interval between the emission and reception of the laser signal allows the assessment of the distance between the instrument and the surveyed point. According to this principle, TLS is employed to collect a dense array of laser distance return values, which are gathered into highly accurate, digital 3D models that can be also transformed into digital elevation models (e.g., Walsh et al. 2018). Several applications of TLS are commented in the scientific literature, with specific reference to rock mass mapping in underground works (Monsalve et al. 2019) or cultural heritage sites (Mineo et al. 2018), to monitor the rock deformations (Abellán et al. 2013; Pratesi et al. 2014) or to evaluate the rockfall hazard (Lato et al. 2012; Gigli et al. 2014a, b). The main advantage of this surveying methodology is its accuracy (millimetric order), which is function of both the distance scanner-target and the ray angle of incidence.

The employed instrumentation is a 3D Stonex X300 Laser Scanner, with a full panoramic horizontal angle and an acquisition rate of 40 k points per sec. For a detailed reconstruction of the cliff morphology, 7 surveying points were chosen both at the foot of the cliff and on the main square. About 43 million of points were processed to achieve a Digital Terrain Model (DTM) of the cliff. Data surveyed by TLS have been coupled with the photos acquired by an unmanned aerial vehicle to obtain a realistic textured model of the slope.

Infrared thermography applied to the geomechanics

Infrared thermography is a non-destructive survey methodology allowing the assessment of the surface temperature of a body, which emits thermal radiation. In nature, all forms of matter with temperature above the absolute zero emit thermal radiation, which is characterized by wavelengths between 0.1 and 100 μm in the electromagnetic spectrum (mainly falling in the infrared band) (Hillel 1998). Thermal radiation is not visible by the naked eye, and its intensity is proportional to the temperature of the emitting material according to Stefan- Bolzmann's Law (e.g., Hillel 1998; Meola and Carlomagno 2004; Shannon et al. 2005 and references therein)

$$J = \varepsilon \sigma T^4$$

where J is the total energy emitted by the surface of an object across all the wavelengths, σ is the Stefan–Boltzmann constant, ε is the emissivity, and T is the temperature of the emitting material.

Thermal cameras are specific devices, operating in a range of wavelengths up to 14 μm through clear air (e.g., Rees 2001), capable of building color-scale images (thermograms) according to the

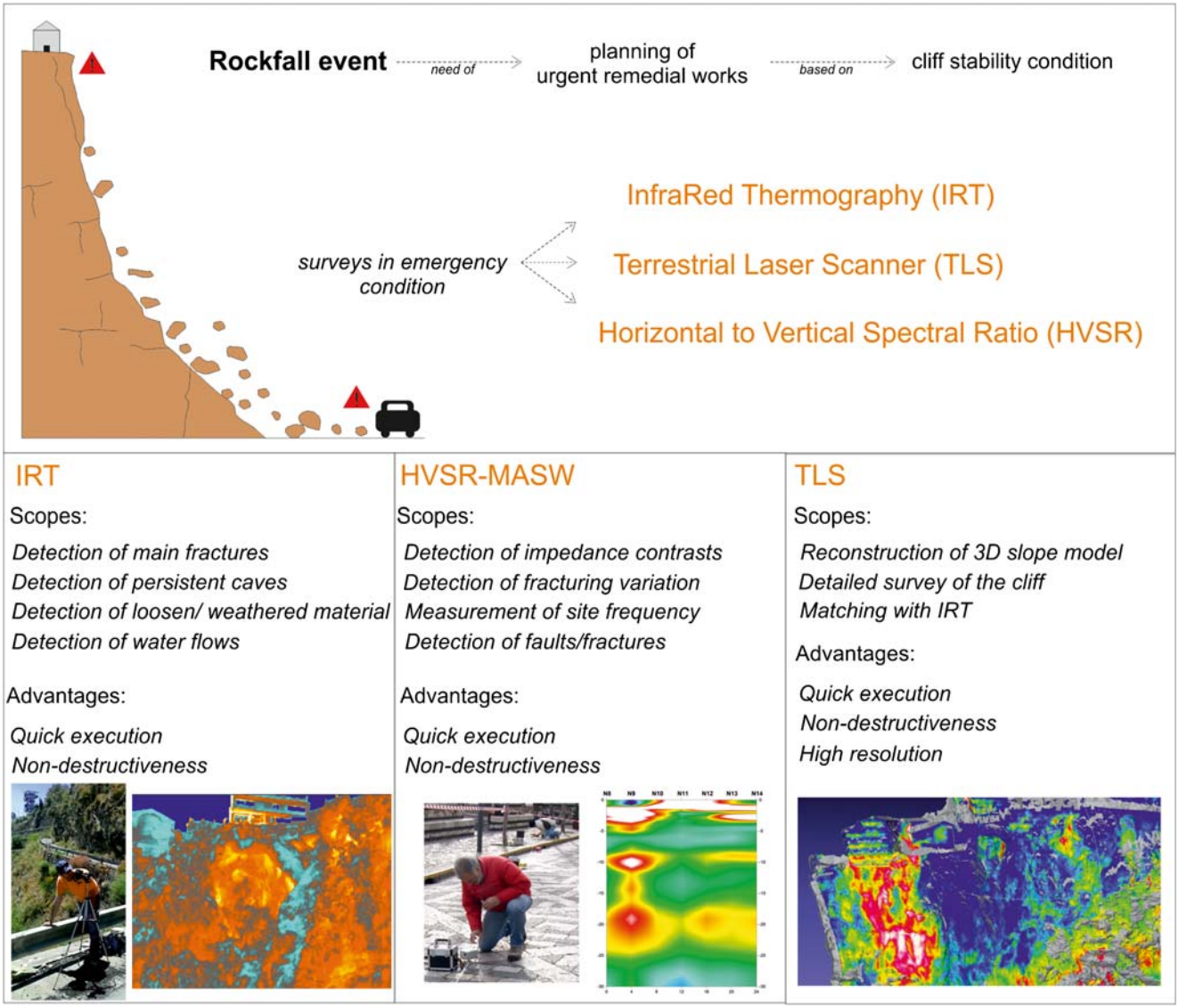

Fig. 5 Summary of the methodological approach followed for this study, applied in emergency condition to study a rockfall event and its potential evolution

surface temperature variation of the framed subjects. This is a quick way to represent in the visible field, something that is invisible to the human eye.

In the latest years, IRT proved a promising tool for the study of severe engineering geological and geomorphological subjects, such as landslides (e.g., Squarzoni et al. 2008; Mineo et al. 2015a; Teza et al. 2012; Casagli et al. 2017; Frodella et al. 2017a, b; Pappalardo et al. 2018a). With specific reference to rock masses, the analysis of the rock fracturing can benefit from IRT surveys, as the distribution of thermal anomalies proved well correlated with open fractures and loosen material (Mineo et al. 2015b). Wu et al. (2005) applied this technique to assess the integrity of a rock mass behind a shotcreted slope, demonstrating that the spatial distributions of large temperature increment is compatible with the existence of eroded caves. Baroň et al. (2014) employed IRT to map open fractures along unstable rock slopes in Czech Republic and Austria, while Gigli et al. (2014a, b) employed it as a support tool for the stability analysis of rock masses in Italy. Pappalardo et al. (2016a) proved the utility of an IRT monitoring during the cooling phase of rock masses, establishing the Cooling Rate Index (CRI) for a direct correlation with the degree of fracturing of the rock. Such experimental application, which returned satisfactory results even for hydrogeological purposes (Pappalardo 2018), was also tested in laboratory to study texture and porosity of intact rock specimens (Mineo and Pappalardo 2016a, b, 2019; Pappalardo and Mineo 2017), providing a satisfactory relationship between CRI and porosity. All these recent applications, followed by promising results, suggest that IRT owns a good potential in the remote survey of rock masses. For this reason, a high-sensitivity infrared thermal imaging camera, with a 320 × 240 pixels infrared resolution and operating in a range of temperature from − 20 to 650 °C (with ± 2 °C accuracy) was employed for the IR study of the unstable cliff. According to literature data (FLIR 2015; Pappalardo et al. 2016a), emissivity was set to 0.93 for the

thermograms processing, which proved a suitable representative value for the remote IRT surveying of an extensive part of slope where different "elements", characterized by different emissivity values, coexist (e.g., bare rock, vegetated sectors, talus, anthropic features). The IR analysis of the unstable cliff was carried out from two frontal survey spots located 230 and 45 m away from the rockfall site, from now on referred to as shooting points 1 and 2, respectively.

The horizontal to vertical spectral ratio technique

The HVSR survey is a non-invasive and fast passive seismic technique used to estimate site resonance frequencies (Nogoshi and Igarashi 1970; Nakamura 1989).

Starting from the acquisition of environmental noise (Okada 2003) in its three spatial components, this technique allows achieving a frequency spectrum, specific for the site (Fig. 6a), which is characterized by one or more peaks. Such peaks can be correlated to some specific features of the subsoil, such as discontinuities, which cause a change in its properties (for example lithological variations or variation in the geomechanical properties of the rock), thus allowing the seismo-stratigraphic reconstruction of the subsoil.

The feasibility of this method applied to specific sites, showing a subsoil affected by different lithological units or lithologies with dissimilar geomechanical characteristics, has been extensively studied and tested in recent years. For example, passive seismic surveys were successfully applied to the study of landslides with specific reference to the identification of the sliding surface depth (Danneels et al. 2008; Imposa et al. 2017a) and, in some cases, also monitoring variations over time (Amitrano et al. 2007; Imposa et al. 2007b). It is indeed reasonable to expect that a landslide body is characterized by different physical-mechanical features with respect to the underling layer; this contrast of properties is detected by HVSR as an impedance contrast.

This technique is based on the assumption, in terms of subsoil stratigraphy, that a layer is a distinct unit separated from those above and below it by an impedance contrast, i.e., the ratio between the seismic impedance between the layers.

Such contrast may be related to stratigraphic variations (Amorosi et al. 2008), intended also as an alternation between intact and fractured layers of a single lithology (Gross 1995). Therefore, the H/V single-station technique can provide information also about changes in the degree of fracturing of the rock sequence (Pappalardo et al. 2016b), i.e., the impedance contrast occurs between layers with different geomechanical characteristics.

Each peak in the H/V spectrum corresponds to a possible seismo-stratigraphic level presenting an impedance contrast compared with the neighbor levels.

In a simple two-layer system, composed by a soft layer above a bedrock, the relationship linking the fundamental resonance frequency f to the thickness of the overlying layer H is given by the following equation:

$$f = Vs/4H \tag{1}$$

where Vs is the shear wave velocity in the investigated medium.

It is reasonable to assume that the shear waves velocity in the subsoil increases with depth, due to the increase of the lithostatic load. According to the following function (Ibs-von Seht and Wohlenberg 1999), once known, the trend of shear

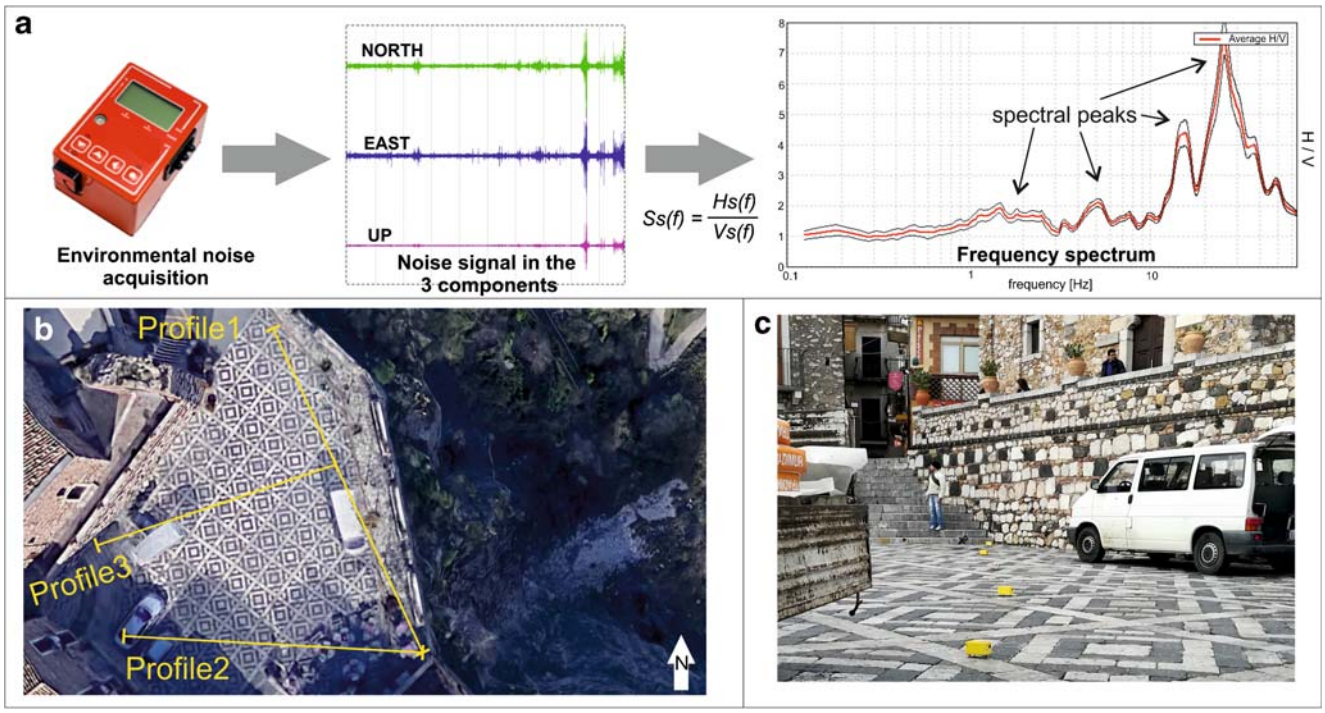

Fig. 6 **a** Sketch of the procedure followed for the acquisition end processing of the environmental noise; **b** location of the measuring alignments on the square; **c** field setting during the acquisition stage along profile 3

waves V_s with depth Z (obtained by a multichannel seismic survey MASW):

$$Vs(Z) = Vo(1+Z)\alpha \quad (2)$$

V_o (shallow shear wave velocity) and α (proportionality coefficient between depth and velocity) parameters, for which there is the minimum misfit between the experimental V_s–depth profile and curve fitting these data, can be obtained.

These two parameters can be used to turn the frequency f into depth values h, according to the H/V spectra, by Ibs-von Seht and Wohlenberg's formula (1999):

$$h = \left[\frac{V_o(1-\alpha)}{4f} + 1\right]^{1/(1-\alpha)} - 1 \quad (3)$$

If the environmental noise samplings are performed at regular spacing, it is possible to reconstruct the impedance contrast sections by using a contouring algorithm. The x-axis in these sections shows the horizontal length along the aligned measuring points placed on the ground, while the y-axis is for depth. The distribution of the amplitude values of the H/V spectral ratio is represented by colors associated with a chromatic scale.

In order to assess the possible presence of directional effects, data obtained by the HVSR analysis were processed with the DHVPOR (directional H/V peak occurrence rates) technique (Del Gaudio et al. 2008, 2013). This allows highlighting a systematic direction in site response, through the observation of a high percentage of peaks H/V around a given frequency and a given azimuth. The DHVPOR analysis allows distinguishing, with a good statistical significance, the directional effects, which are closely related to the structural and geo-lithological properties of the subsurface.

The average values of the H/V spectral ratios for azimuthal intervals of 10° and frequency intervals of 0.5 Hz were calculated. The analysis took into account only the H/V peaks characterized by an H/V ratio average value greater than 2 and H/V maximum and minimum ratios observed at the same frequency (in an orthogonal direction with divergence no more than 30°) at least equal to 1.5 (Del Gaudio et al. 2008, 2013). The occurrence rates were evaluated in the frequency range 0.5–20 Hz. This technique put in evidence the percentage of time windows, for each acquisition, characterized by directional peaks, with a similar orientation, in order to highlight the site directional resonance properties. Furthermore, these occurrence rate percentages were plotted on 3D histograms where the vertical bars height is proportional to the occurrence rate percentage, for each frequency–azimuth combination.

On the main square, 19 environmental noise samplings were carried out along three different profiles having one common measuring point. In particular, profile 1 was parallel to the cliff face, while profiles 2 and 3 had a perpendicular orientation to allow the investigation of the inner portion of the rock mass below the main square (Fig. 6b). Each profile consisted of 4 m spaced measuring stations (portable digital three-components seismographs (Fig. 6c), with a sampling frequency of 128 Hz, for 20 min) recording the environmental seismic noise. During the acquisition phases, the vehicular traffic was inhibited to avoid any source of disturbance on the recorded signals. A multichannel analysis of surface waves (MASW) was performed to estimate the shear waves velocity profile within the subsoil (Park et al. 1999), according to Eq. 2 and the related methodological approach reported in the previous sections. The 28-m long MASW alignment was parallel to the cliff, and the seismic signal was acquired through a digital multichannel array, equipped with 14, 2 m spaced, vertical geophones with natural frequency of 4.5 Hz. An 8-kg hammer beating on a metallic plate, placed 4 m away from the geophone starter, was used for energization. In order to gain a signal with an energy content higher than the ambient noise, the stacking technique was applied; it consists in carrying out several energizations at the same point.

The acquired signal has been analyzed in the frequency–phase velocity domain. Once the dispersion spectrum of Rayleigh waves from the MASW elaboration was attained, a joint fit between the dispersion curves and one among the most representative H/V spectra was performed. The joint fit procedure allows a better constraint of the Vs-depth profile (Castellaro and Mulargia 2009). The parameters of the starting subsoil model (Vs, Vp, thickness, density, Poisson ratio) are reiteratively modified to minimize the misfit between the experimental curves (dispersion curve and H/V spectrum), obtained from the surveys processing, and the theoretical ones calculated by the subsoil model. The model affected by the lowest misfit it is the most reliable in terms of seismo-stratigraphic conditions of the subsoil.

Results

Rock mass characterization and 3D model by TLS

Although the geomechanical features of the rock masses in the area are known, for this research, a specific survey of the cliff affected by the 2019 rockfall was performed by experienced climber surveyors. Surveyed discontinuities show a great rate of dispersion index of the high degree of fracturing arising from a peculiar tectonic history of this area and can be grouped into 7 systems (Fig. 7).

Two main source areas can be identified (Fig. 7a). From a kinematic point of view, the 2019 one is an asymmetric wedge formed by two intersecting systems. The unstable rock volume slid along a dip-slope plane 085/65 leaving a cavity under the banister and pavement of the main square. On the other hand, the largest source area (about 260 m^2) belongs to one or more not specified rockfall events (among which the one occurred in 2015, whose blocks and debris are still present at the foot of the cliff) and occurs a few meters below a public edifice of the main square (Fig. 7a). An 8.5-m high and 5.5 m large karst cavity occurs along a fracture trace (F1), which at a closer observation shows a series of streaks suggesting a tectonic origin of this discontinuity (Fig. 7b). The discontinuity orientations, acquired during the rock mass survey (Fig. 7c), allow stating that this source area is a wedge formed by the intersection of 3 sets and, although part of the rock volume has already failed, there are signs of further material in precarious stability conditions. Therefore, a limit equilibrium analysis was performed according to both surveyed and literature data (Pappalardo et al. 2014), and a 0.63 factor of safety was estimated in static conditions, proving the persisting instability of this sector of cliff (Fig. 7d). All these elements are clearly

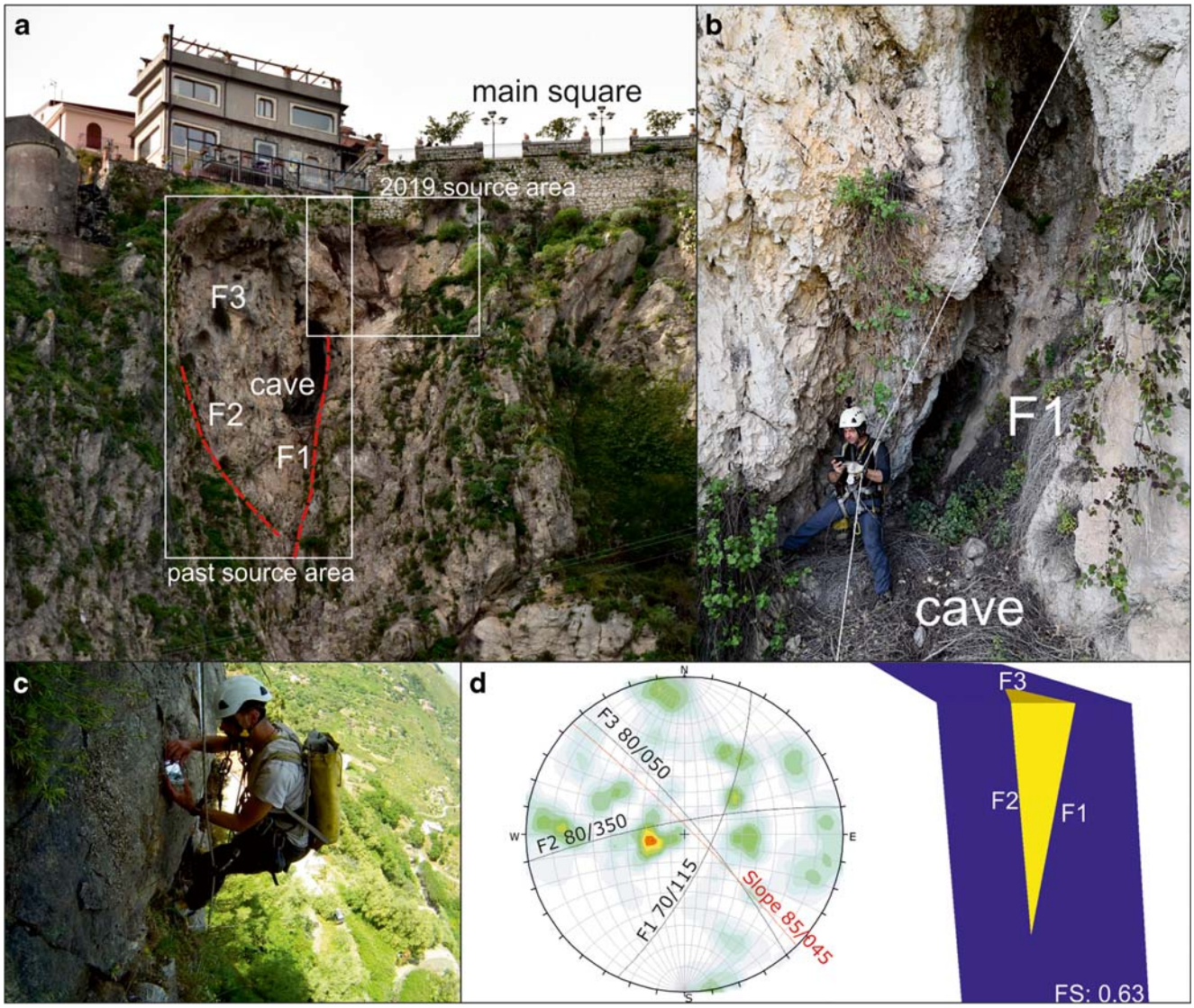

Fig. 7 **a** Surveyed cliff with the main elements under investigation highlighted; **b** particular of the cave during the rock mass survey; **c** rock mass survey phase; **d** geostructural data and 3D model of the wedge within the past source area (the factor of safety FS was estimated by limit equilibrium analysis)

recognizable on the 3D model of the cliff achieved by the TLS survey (Fig. 8a), where the talus of all the past rockfalls occurred at this sector can be mapped. The model shows also the presence of a shear plane at the foot of the cliff affecting the Triassic formation of limestone and dolostone (dashed line in Fig. 8b). This shear plane seems to be crossed by a tectonic structure, with a direction likely similar to F1, which causes a throw visible in the model. Above this plane, a further protruding rock volume stands below the 2019 source area. Its evidence is poor in the model due to the presence of vegetation, but its unstable condition must be reported. In fact, the dip slope geometry of the shear plane suggests a kinematically hazardous incipient movement involving about 450 m^3 of rocks (white rectangle in Fig. 8b). Furthermore, this volume is sided by the presence of cavities developed along the aforesaid tectonic structure with direction similar to F1, which can be regarded as enhancement features of a forthcoming instability.

Infrared thermography mapping of the rock cliff

From a frontal survey spot, an overview on the whole cliff is achieved. Due to the peculiar orientation of the rock face, with sudden changes caused by the tectonic setting of the area, the cliff suffers a non-uniform insolation condition. In fact, the highest surface temperature affects the SE-facing portion of the cliff due to the direct insolation (the IRT image was taken at noon), while the coldest temperatures affect the shadowed portions comprised between the NE and E-facing rock faces (Fig. 9a). In this shadowed sector, two positive anomalies (higher surface temperatures) represent a hollowed rock mass sector, corresponding to the two main rockfall source areas previously defined. These are labeled with a slightly higher surface temperature due to the preservation of a warmer temperature, not perceptible to the naked eye (Pappalardo and Mineo 2019 and references therein). Such emptied zones are surrounded by negative anomalies (i.e., lower surface

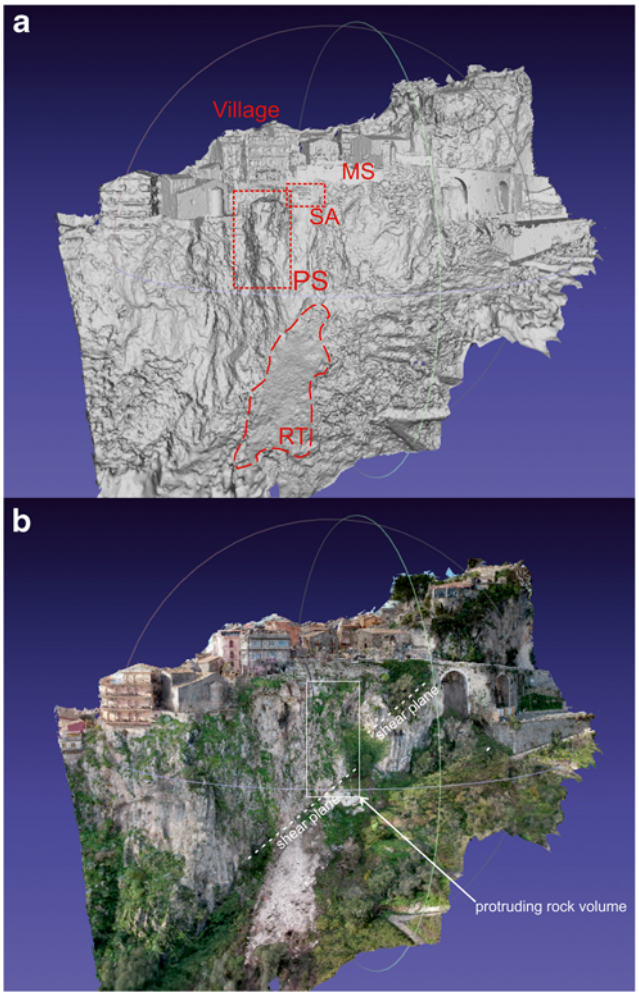

Fig. 8 3D mesh obtained by TLS survey: **a** raw mesh of the studied cliff with labels of the main elements (MS, main square; SA, 2019 source area; PS, past source area of 2015 and previous undefined events; RT, rockfall talus of 2019, 2015 and undefined past events); **b** 3D model of the cliff with a texture arising from aerial photos acquired by an unmanned aerial vehicle

temperatures) referred to protruding rocks and/or presence of water. By filtering the temperatures of this cliff sector in the range 4–8 °C, the two main source areas can be well identified, along with the deep cave highlighted by the strong contrast of temperature. In fact, Pappalardo et al. (2016a) after a rock mass monitoring demonstrated that when the rock mass is directly irradiated by sunrays, cavities maintain by a lower temperature with respect to the surrounding more exposed rock mass sectors. On the other hand, when the rock mass is in shadow condition, such as the case of the rock mass portion analyzed herein, cavities, along with open cracks, hold a higher surface temperature and can be easily identified (Fig. 9b). In this case, the utility of IRT is in the discrimination of persistent and shallow cavities. In fact, several other cavities occur along the cliff and were identified by IRT as they are marked by positive anomalies. These are located along the main tectonic structures (e.g., faults), where water circulation enhances dissolution phenomena (Fig. 9a). The colder zones surrounding this large hexagonal source area are index of protruding rock mass portions and water flows on the rock face (Fig. 9c). In fact, according to the direct observation of the cliff face by climbing surveyors, we could assess that the lowest temperature is related to wet rock surface. The identification of protruding portions, in this case labeled by negative anomalies, is a key activity, as these represent unstable material potentially involved in future rockfalls, while the presence of water can be addressed as a predisposing factor of a landslide event. This gains specific relevance considering that such water flows probably originates from the upstream edifices.

The 2019 source area occurs at the highest sector of the cliff, where a positive thermal anomaly highlights the hollow rock mass portion emptied by the latest event. This shows a peculiar kinematic pattern, as it is enclosed between two intersecting discontinuities giving rise to a wedge configuration, as already highlighted by the survey. The intersection of such systems occurs along the entire studied cliff, as highlighted by IRT (Fig. 9d). This is a key interpretation of the widespread instability, which is driven by a series of wedge patterns of different orders, as already highlighted by previous studies in this area (e.g,. Mineo et al. 2017; Pappalardo et al. 2017). Wedges are usually formed by two or three intersecting discontinuity sets; in the latter case, two traces are visible along the slope face and the third is a dip-slope plane acting as tension crack. The sliding occurs either along the dip-slope plane or along one lateral discontinuity plane, as occurred for the 2019 event.

The second surveying spot, located at the foot of the cliff, allows a detailed remote survey of the upper portion of the cliff (Fig. 10a), where the 2019 rock volume detached leaving a cavity below the main square of the village. The analysis of IR images (Fig. 10) highlights the persistent aspect of the cavities occurring within the past source area (the one with hexagonal shape in Fig. 8). In particular, the highest surface temperature is found at the largest opening, suggesting a deep prosecution of the cavity in depth. In this perspective, the higher the surface temperature, the deeper the cave. This is a relevant feature to highlight, as it testifies the occurrence of karst processes, which plays a weakening action on the mechanical behavior of a rock mass and can lead to instability phenomena (e.g., Santo et al. 2007; Saroglou et al. 2012; Niu et al. 2015). This consideration is even supported by the detection of certain rate of water flowing along the rock face (Fig. 10a), which enhances the carbonate dissolution process. By filtering the temperatures within a 6.2–4 °C range, the crown belonging to both previous and the 2019 events can be easily defined (Fig. 10b). In particular, the 2019 crown is limited by the cantilever foundation of the main square, which represents the main current element at risk. On the other hand, the upper boundary of the past source area is represented by a protruding rock mass highlighted by a negative thermal anomaly. Among the hollowed sectors highlighted by higher temperature in Fig. 10a, the two deepest cavities are further highlighted in Fig. 10b. By enhancing the contrast between higher and lower surface temperatures (Fig. 10c), which highlights that such protruding rock mass is overleaf limited by an open discontinuity marked by a liner positive thermal anomaly. This suggests a loosening of such rock mass, probably due to a progressive stress relief after the loss of the underlying rock support, which can be now regarded as a prone-to-fail rock volume needing immediate stabilization works (Fig. 10d).

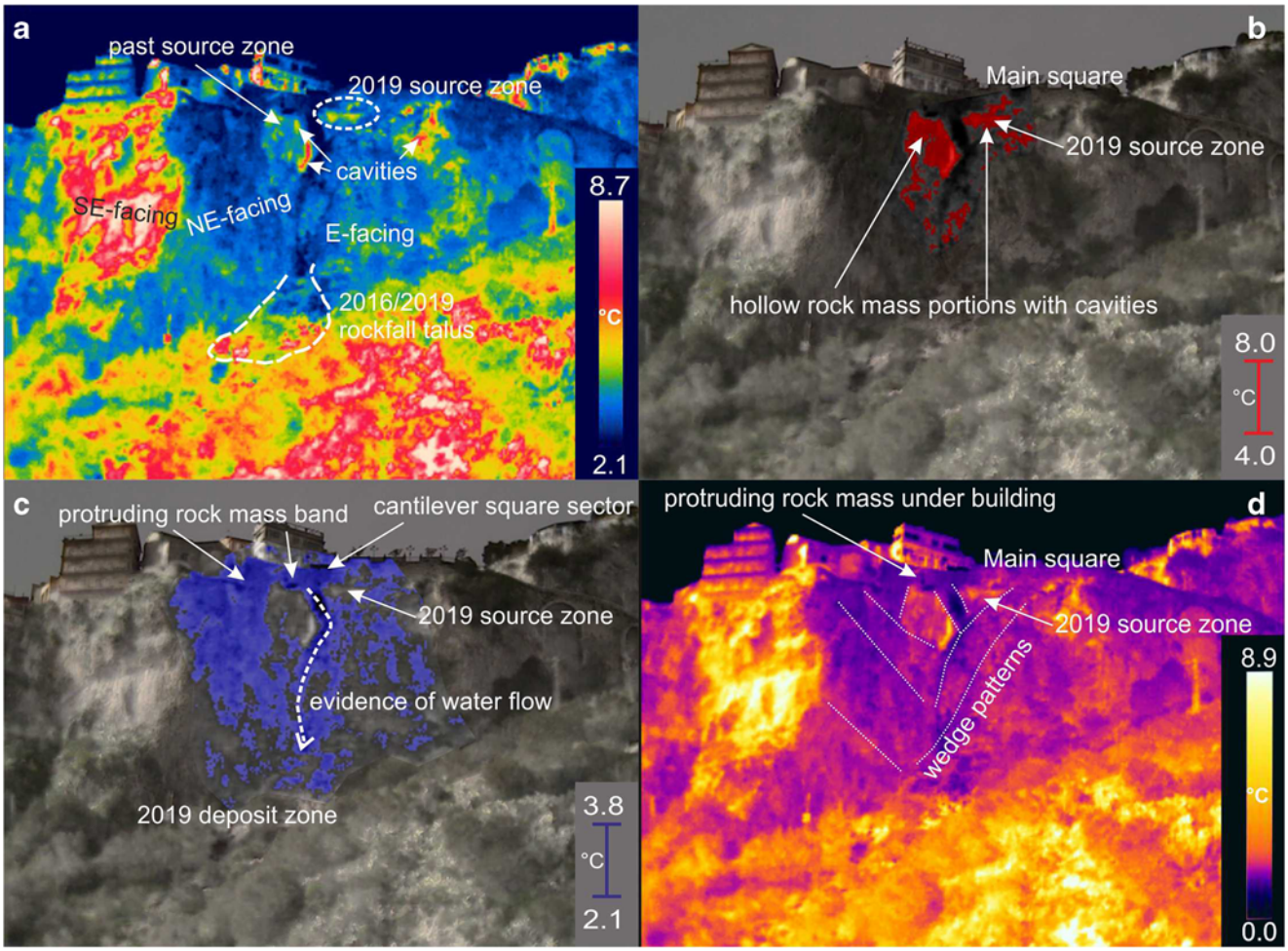

Fig. 9 IR images of the cliff taken from survey point 1: **a** peculiar elements highlighted by IR; **b** range of temperature 8–4 °C highlighting the hollow rock mass portions; **c** range of temperature 3.8–2.1 °C highlighting protruding rock mass sectors and water flow; **d** main geostructural elements of the cliff highlighted by IRT

Geophysical survey

The 1D Vs-depth profile (Fig. 11) shows a normal velocity pattern characterized by a significant increase of shear waves velocity with depth. The V_o and α values, obtained by the fit of Vs-depth profile (Fig. 11), for which there is a minimum misfit between the data of the profile and the Eq. 2 with which the fit of such data was made, are equal to the following: $V_o = 150$ m/s; $\alpha = 0.45889 \pm 0.01743$ (3.799%).

According to Ibs-von Seht and Wohlenberg's formula (1999) (Eq. 3), H/V spectra frequency values were converted in depth, and values of each H/V measuring points (Fig. 12a) were interpolated to reconstruct the impedance contrast sections.

Section 1 (parallel to the cliff face) (Fig. 12b) shows a first strong horizontal impedance contrast (IC1) at about 2 m of depth, probably related to the transaction between the filling material used for the construction of the square and the underlying rock. IC1 occurs also in the other two impedance contrast sections, at about the same depth (Fig. 12c, d). Two further significant horizontal impedance contrasts (IC2-IC3) occur at about 10 and 20 m of depth in all the sections. Considering that no geological variations along the exposed cliff face are visible at this depth, such contrast is likely related to a transition between rocks with variable physical-mechanical characteristics due to a different degree of fracturing.

An interesting outcome is the presence of a vertical impedance contrast (IC4) occurring at sections 2 and 3, well visible in the depth interval 5–25 m. Such contrast is found 4 and 12 m away from the cliff edge at sections 2 and 3, respectively (Fig. 12). This suggests the presence of a vertical structure crossing the sections at about N9 and N17 sampling points. A reasonable interpretation of this outcome is the presence in the subsoil of a mechanical discontinuity (crack, joint, fault), which crosses the main square, with a direction well matching with the F3 discontinuity surveyed along the cliff and driving the instability of the wedge within the past source area. Due to the relevance of this outcome, which could play a key role in the stability of the main square in case of cliff retreat, we have investigated on the directional effects found at some noise measurement points. The occurrence rates of some environmental noise recordings along the different alignments are shown in Fig. 13. The directional effect affects the frequency range in which the resonance peaks fall. By analyzing the 3D histograms,

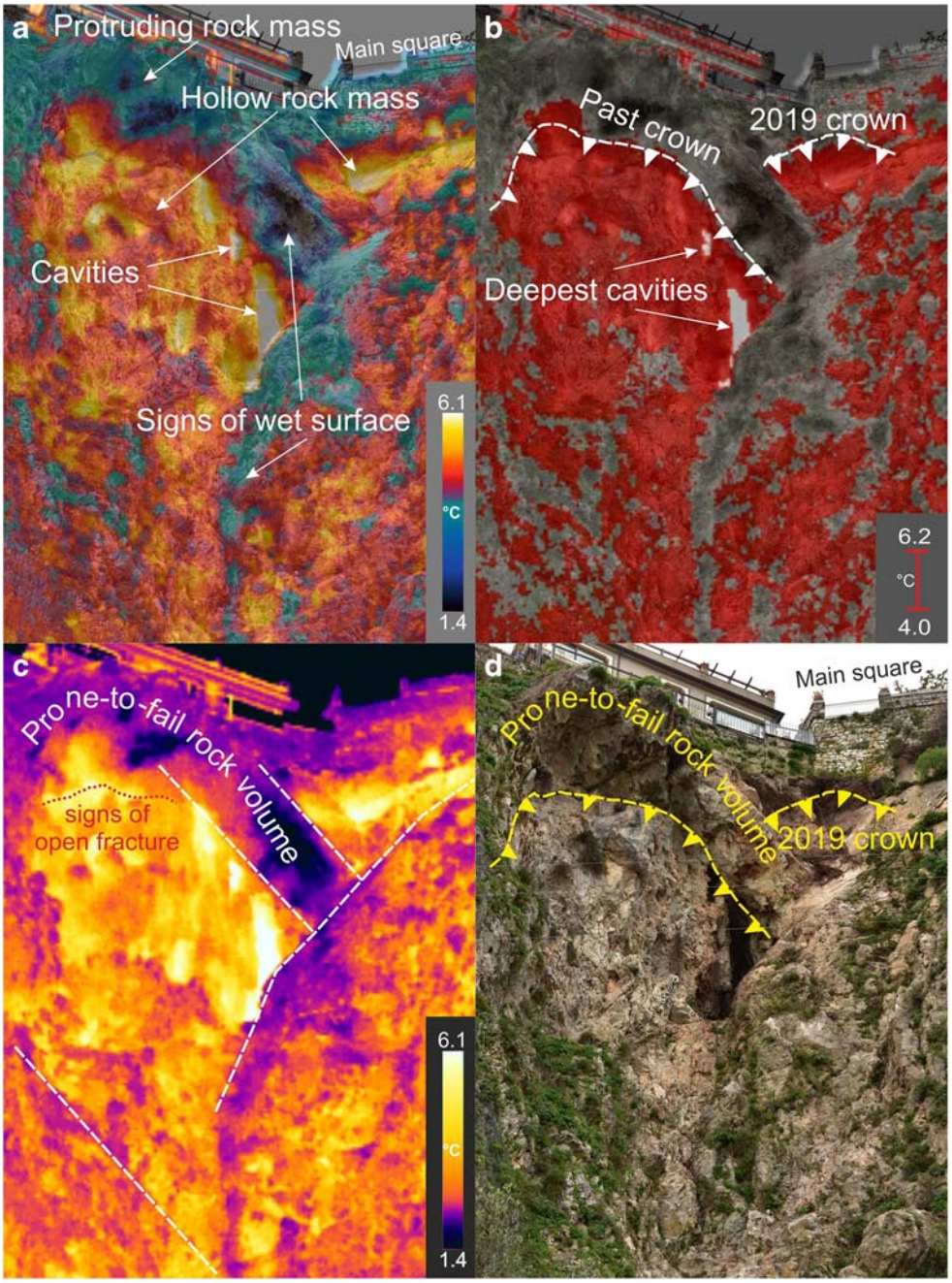

Fig. 10 IR images of the upper cliff taken from survey point 2: **a** cavities and protruding rock highlighted by IR; **b** range of temperature 6.2–4 °C highlighting the crowns of rockfall events; **c** prone-to-fail rock volume and signs of open overleaf fracture; **d** digital picture of the framed area with highlighted the main recognized elements

two different directional effects, affecting two different ranges of frequency, can be noted. In particular, N3 and N9 measuring points (Fig. 13a, b) show at high frequency an azimuth between 100° and 140° N; the occurrence rate percentage is around 75% at N3, which is the closer to the edge of the cliff, and around 40% for N9 point (Fig. 13a, b). Such directional effect can be related to the topographic effect induced by the proximity of the edge of the cliff with reference to the sampling points.

The second directional effect shows an azimuth between 30° and 50° N at low frequency, and the associated occurrence rate percentage is around 30–40% for both recordings. A similar effect was found even at the N14 and N17 sampling points, characterized by a single directional effect, with azimuth between 30° and 50° N, affecting the entire frequency range of the resonance peaks (Fig. 13c, d). The highest occurrence rates percentage is around 30–40% for both recordings. The percentage values of the occurrence rate for particular frequency–azimuth pairs (30–75%) highlight that there was a constancy of the directional peaks during the sampling, thus a directional order at specific frequencies in the local seismic response. This kind of effect, which typically occurs

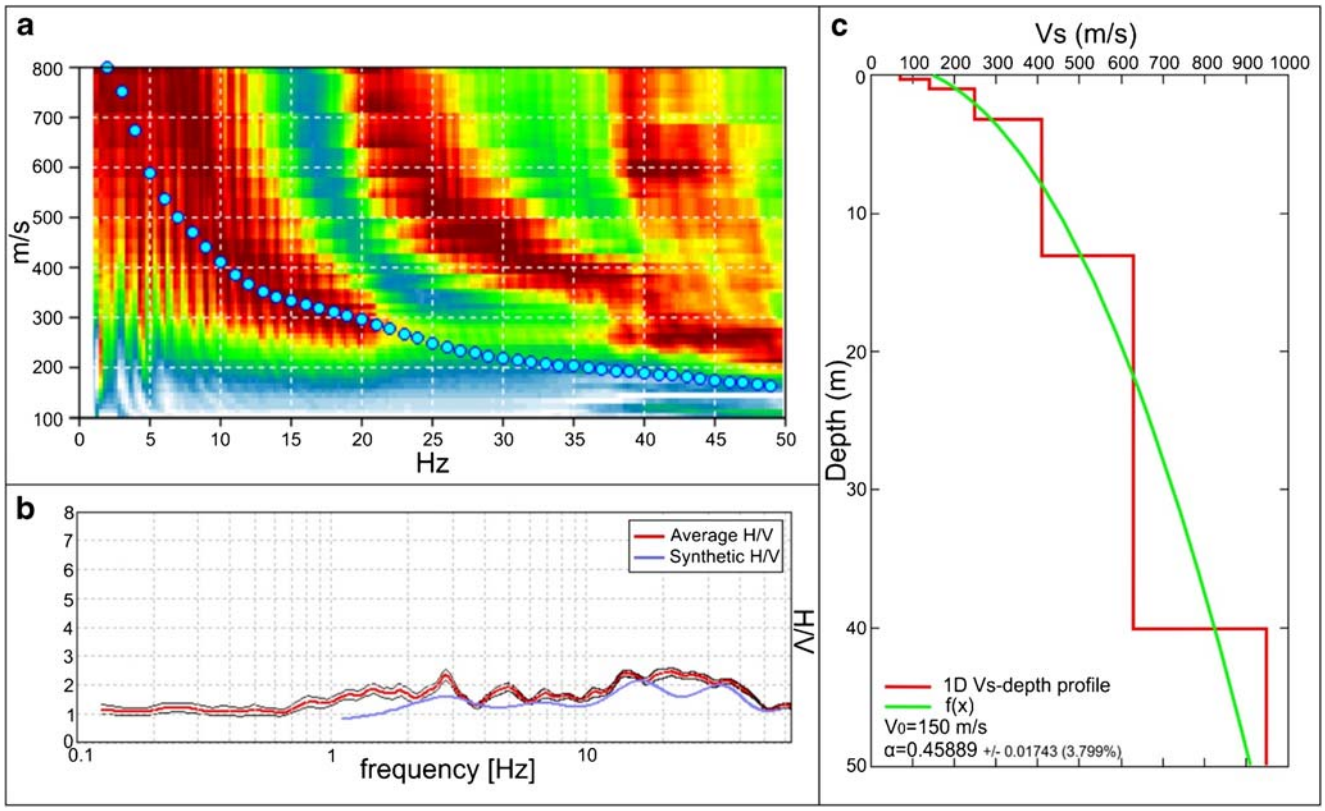

Fig. 11 **a** Rayleigh waves dispersion curve obtained from the MASW survey; **b** HVSR spectrum, relating to N5 environmental noise record; **c** 1D velocity–depth profile obtained from MASW-HVSR joint fit: the green curve represents the function $Vs(Z) = V0\,(1 + Z)\,\sigma$ that has the minimum misfit with the data of the 1D Vs–depth profile

close to a tectonic structure (Imposa et al. 2004; Pappalardo et al. 2018b), proves the presence of a discontinuity in the subsoil, which can be related to F3.

Discussion and conclusions

A combination between non-invasive surveying methodologies has been herein presented with the aim of a quick evaluation of the stability condition of a rock slope in an urbanized area after the occurrence of a rockfall, which caused damages to structures and infrastructures. The innovative integration between infrared thermography, rock mass surveys, terrestrial laser scanner, and horizontal to vertical spectral ratio is focused on the quick detection of the most critical sectors along a rock cliff, in order to achieve technical information for the emergency securing of the area and to address further in-depth surveys for the design of the most suitable remedial works. In fact, IRT and TLS allowed the evaluation of the condition of the rock face through thermal anomalies and point clouds, with hints on the persistence of discontinuities and on the kinematics of potential unstable volumes; on the other hand, HVSR sheds light on the subsoil in terms of impedance contrasts related to either mechanical discontinuities or local peculiar conditions.

To test this surveying approach, the carbonate cliff of Castelmola, one of the most tourist areas of northeastern Sicily affected by a rockfall on 5 January 2019, was chosen. In fact, this event left some critical issues along the slope, because the rock volume detached right below the main square of the village, leading to the instability of the structures above the cliff, and damaged the downstream only access road to the village. This area is not new to rockfalls, and the fair-poor geomechanical quality of the rock masses, along with the complex and long-lasting tectonic history of the area, are among the main causes of this widespread instability. In fact, rock masses are affected by up to more than 5 discontinuity systems, and the main kinematic failure pattern surveyed in the area is the wedge sliding, with wedges formed by the intersection of 2 or 3 systems, sometimes belonging to tectonic structures. This is the case of the 2019 instability, as well as of a source area of past rockfalls, which is enclosed between discontinuities showing also strikes (F1), thus suggesting a tectonic origin of the discontinuities. Moreover, karst caves occur along such planes, confirming the presence of a certain rate of water circulation. More specifically, the past source area is a wedge that still holds unstable rock material, whose estimated factor of safety is 0.63 in static conditions. Furthermore, it is topped by a protruding rock mass portion, which has to be treated as a prone-to-fail volume. Finally, a shear plane at the foot of the cliff was surveyed, index of the intense tectonic disturbance of the slope. The most relevant features were highlighted by employing different remote survey techniques, whose overlapped outcomes returned an innovative and useful IRT-3D model (Fig. 14a). In fact, by spreading the IRT images over the 3D mesh achieved by TLS the past source area is well highlighted by a warm anomaly, as hollow rock portions preserve a higher surface temperature than the protruding ones when the cliff is not directly irradiated by sunrays (Pappalardo

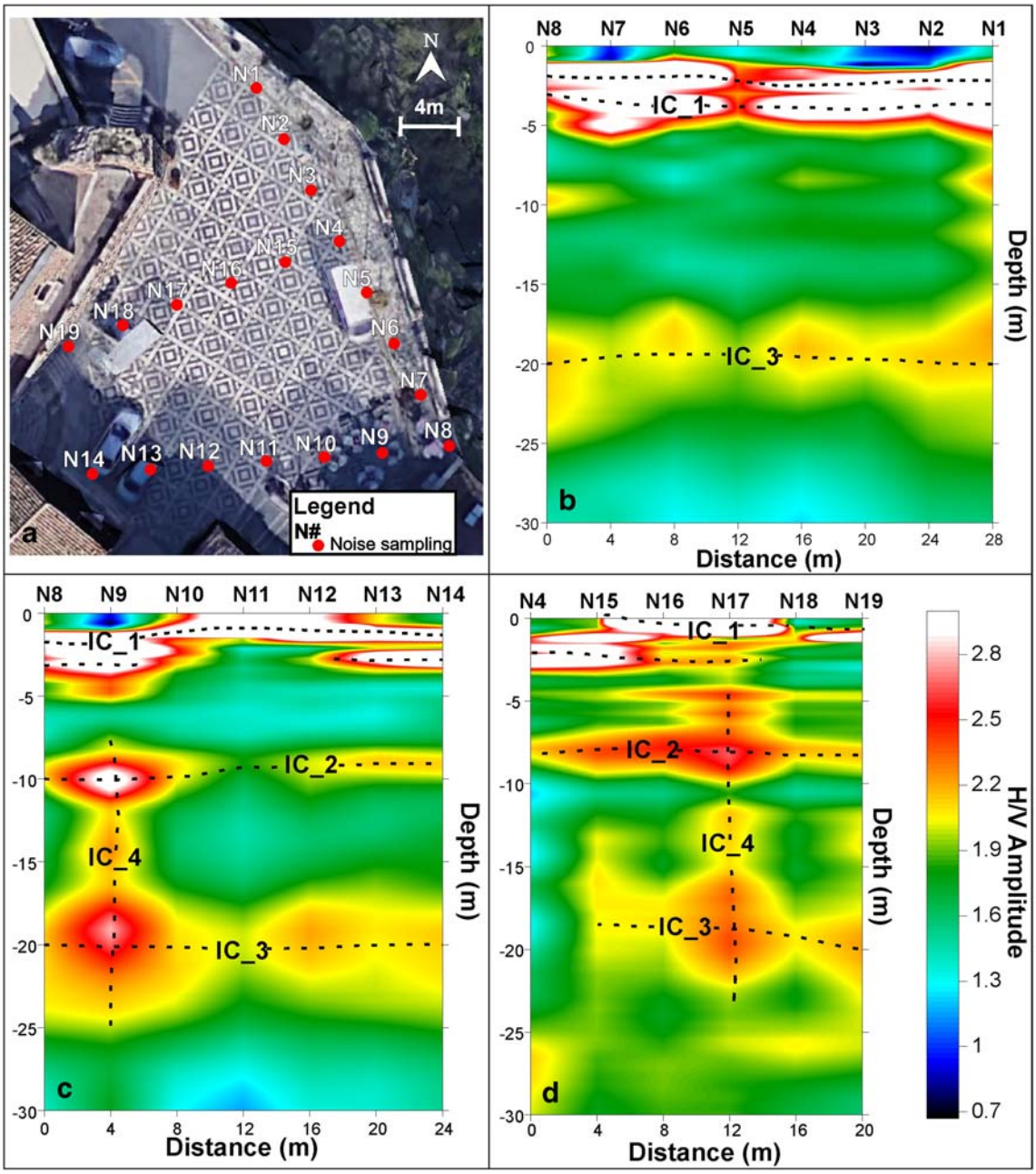

Fig. 12 Location of the environmental noise samplings; **a** photo of environmental noise measuring stations along a survey profile; **b** impedance contrast section 1 parallel to the cliff face; **c** impedance contrast section 2; **d** impedance contrast section 3

et al. 2016a). The source area well defines a wedge shape (Fig. 14b), which is clearly recognizable in the model of the cliff, thus confirming that most of the unstable kinematic features are controlled by wedges. Furthermore, the positive anomalies initially attributed to the presence of persistent cavities, well overlap the cavity traces visible along the cliff. In this case, we found that the deeper the cavity, the higher the surface temperature, based on the temperature contrast between the inner rock mass and the external environment.

Moreover, the protruding rock mass portions above the past source area (Fig. 14b), visible also to the naked eye and highlighted by IRT, was found affected by open fractures bordering its contact with the rock face. These discontinuities are highlighted by positive thermal anomalies, which are more visible by enhancing the contrast of the lower temperatures, suggesting a certain degree of aperture. This suggests, as already hypothesized, the presence of a partially open, sub-vertical crack behind this rock portion (approximate volume 60 m^3), which breaks the continuity of the rock face crossing the entire thickness of the protruding rock volume, thus enhancing its instability. The direction of this element matches with F3 system, proving that the instability of the cliff is linked to the main structural systems of the area.

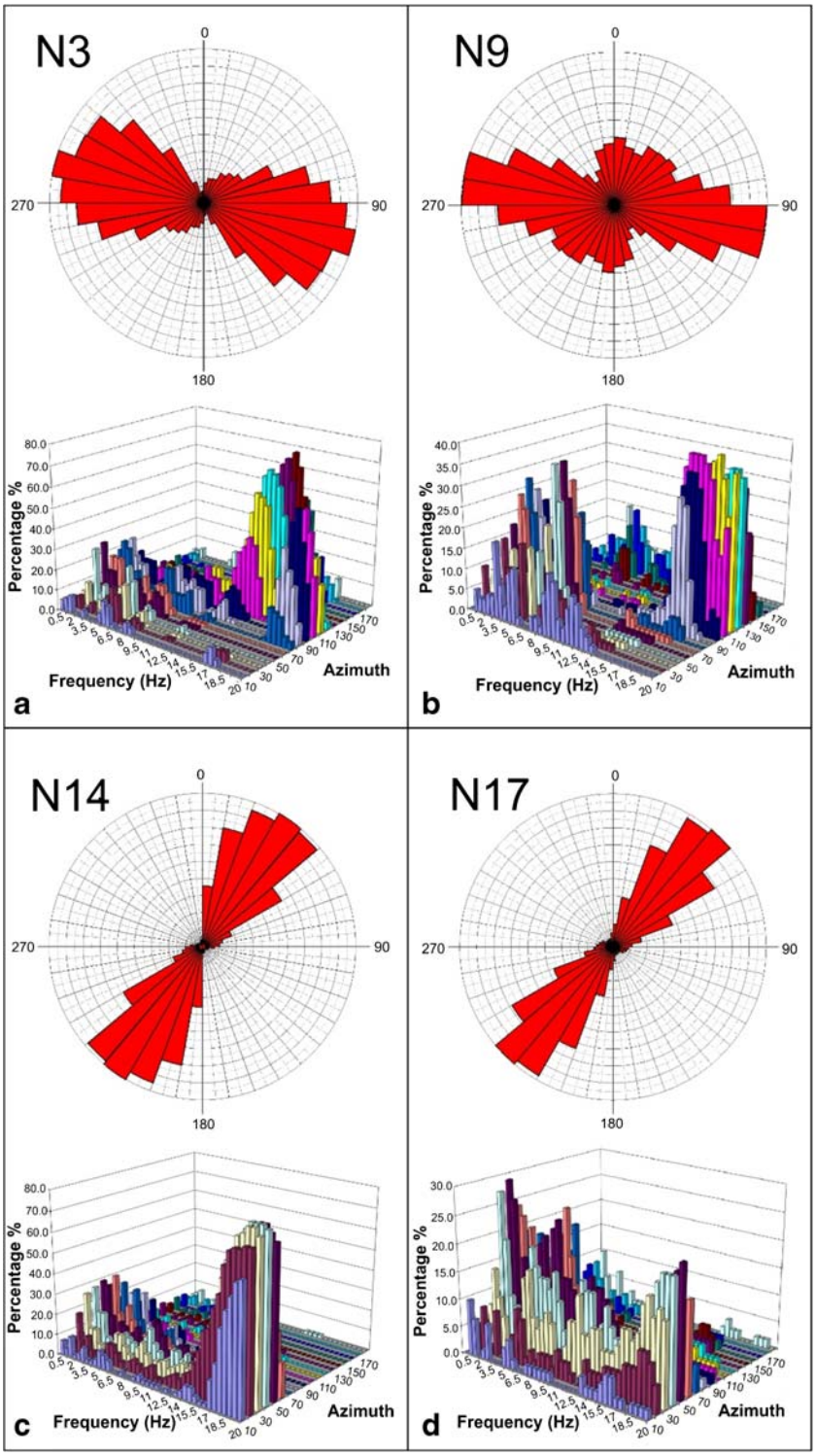

Fig. 13 Rose diagrams of directional effects and histograms of DHVPOR values related to some environmental noise acquisitions carried out in the main square of Castelmola village: **a** N3; **b** N9; **c** N14; **d** N17

All these considerations highlight the actual possibility of future rock detachments, which should be preventively secured. In fact, the occurrence of rockfalls could bring negative effects also on the structures laying above the cliff, such as the main square and the edifices, which should be regarded as elements at risk for cliff retreat phenomena (Fig. 15). In this regard, the HVSR technique shed light on the conditions of the subsoil of the main square, which represents the "inner" portion of the rock mass surveyed by TLS and IRT. Such methodology highlighted the presence of different impedance contrasts in the subsoil below the main square.

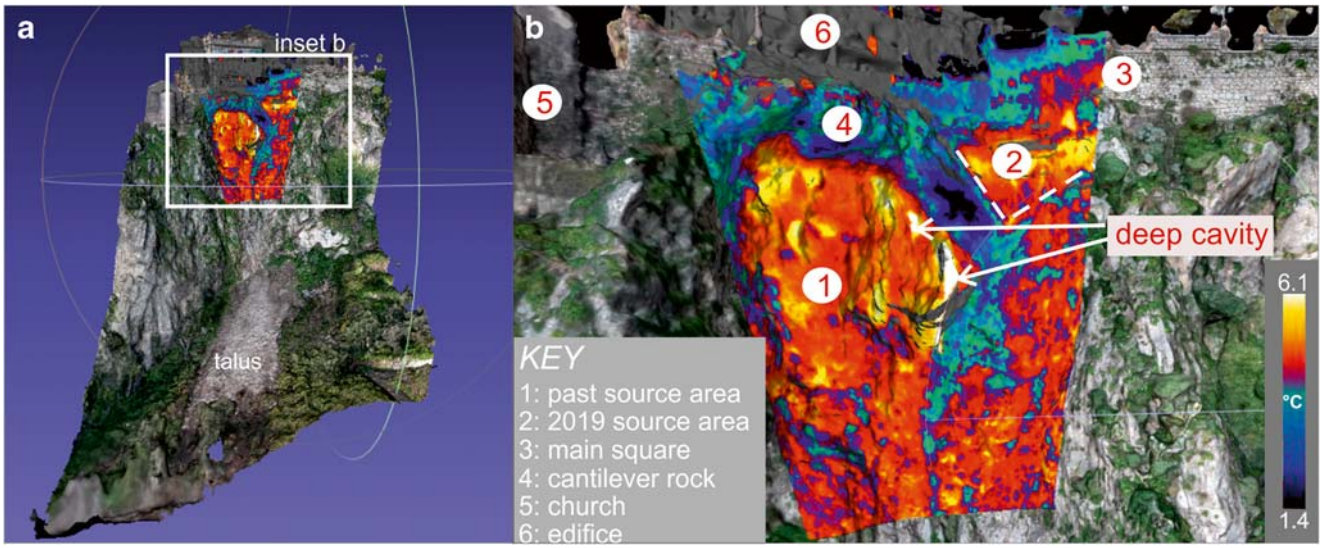

Fig. 14 **a** Example of a IRT-3D model of the cliff; **b** particular of the past source area in the temperature range 1.4–6.1 °C

These are related to a different degree of fracturing of the cliff, which may also condition the hydraulic conductivity of the rock mass. In fact, the karst caves detected along the cliff are located at a depth between − 10 and − 20 m below the square level (matching with the IC2 and IC3 contrasts), which coincides also with the occurrence of the wet rock surface surveyed by IRT. Moreover, a peculiar sub-vertical impedance contrast (IC4) was detected at two specific noise measurement stations (N9 and N17), with a directional effect well matching with the F3 plane surveyed at the unstable wedge. This suggests the presence of a mechanical discontinuity below the main square, probably related to a tectonic alignment, whose likely prosecution would be associated to the dip slope plane (F3) behind the unstable wedge of the past source area (Fig. 15).

Such results prove the highly critical issues affecting this cultural heritage site, as well as the risk arising from potential future rockfalls.

Besides the technical achievements, which surely gain relevance from a local point of view in terms of risk reduction planning, this research presents some interesting scientific outcomes. In detail, IRT further proved its potential in the study of rock masses and in the detection of sectors affected by specific features along a rock cliff (e.g., hollow parts, loose rock, vegetation). It is a reliable tool for the assessment of the relative persistence of cracks and caves, as well as for the detection of water flows, although its application is strictly linked to the availability of suitable surveying point and to the insolation conditions. No particular contraindications can be mentioned in the use of this methodology under different

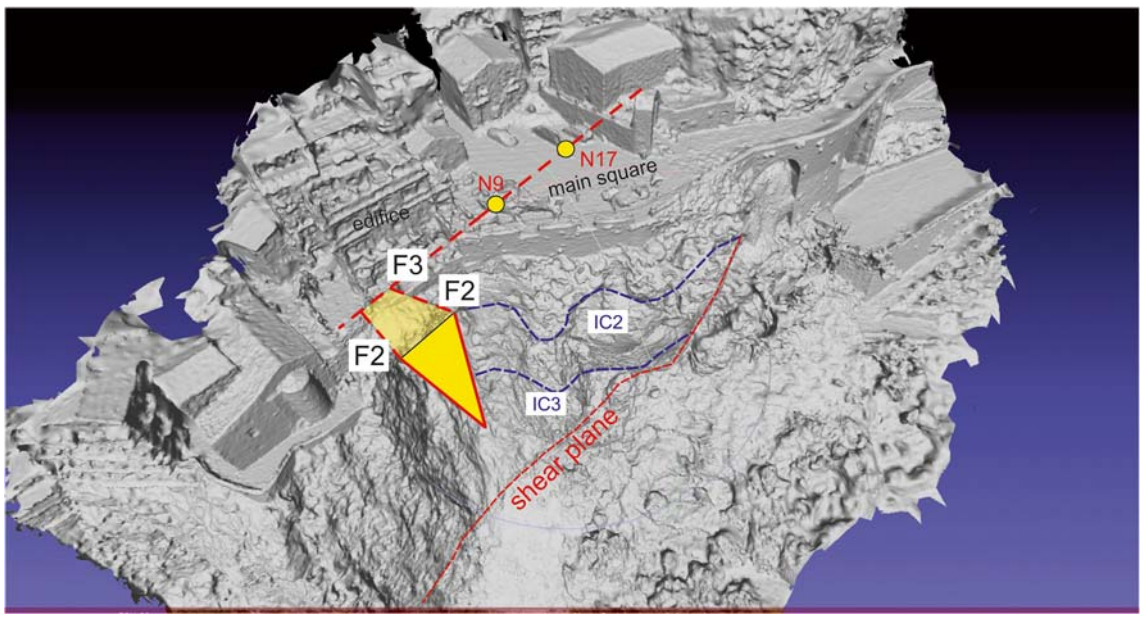

Fig. 15 Summary of the main achievements by the integration of the surveying methodologies presented herein

climatic conditions, although Pappalardo et al. (2016a) reported that the cold weather and slight rain concur in a lower heating of the rock mass during the day, thus resulting in resolution problems (less detailed thermogram). Moreover, the integration of the TLS and IRT remote survey methodologies proved its utility in providing a different way of analyzing both point clouds and thermograms, allowing an easier matching between thermal anomalies and cliff morphology. TLS is a feasible remote survey methodology, which can operate under different weather conditions, although, based on our experience, heavy rain, and fog during the survey can slightly reduce the acquired number of points. Finally, the HVSR technique allowed integrating the structural data surveyed at the rock face with those arising from the impedance contrasts, thus extending the geophysical outcomes to the unstable area detected at the cliff face. Also, this methodology requires portable instrumentations and can be applied under different field and weather conditions, although the direct action of wind and rain on the instrumentation can bring slight vibration affecting the recoded signals. A limitation of this method is represented by the anthropic noise, usually occurring close to roads or crowded places, which overhangs the environmental noise causing troubles with the recorded signals.

All these considerations demonstrate that a quick multidisciplinary approach is the starting point for the study of stability problems, especially during a post-rockfall emergency when the fast achievement of reliable outcome makes the difference in terms of an immediate risk reduction, waiting for further in-depth analyses aimed at the final stabilization of the phenomenon.

Funding information

This work was funded by the Department of Biological, Geological and Environmental Sciences, University of Catania, in the frames of the Piano Nazionale della Ricerca (2017–2020), scientific responsible Sebastiano Imposa, and Finanziamento delle Attività Base di Ricerca, granted to Giovanna Pappalardo.

References

Abellán A, Oppikofer T, Jaboyedoff M, Rosser NJ, Lim MJ, Lato M (2013) Terrestrial laser scanning of rock slope instabilities. Earth Surf Process Landf 39:80–97

Amitrano D, Gaffet S, Malet JP, Maquaire O (2007) Understanding mudslides through micro-seismic monitoring: the super-Sauze (south-east French Alps) case study. B Soc Geol Fr 178(2):149–157. https://doi.org/10.2113/gssgfbull.178.2.149

Amorosi A, Castellaro S, Mulargia F (2008) Single-station passive seismic stratigraphy: an inexpensive tool for quick subsurface investigations. Geoacta 7:29–39

Armesto J, Ordóñez C, Alejano L, Arias P (2009) Terrestrial laser scanning used to determine the geometry of a granite boulder for stability analysis purposes. Geomorphology 106:271–277

AVI Project: Progetto AVI (Aree vulnerate da calamità idrogeologiche), Regione Sicilia Relazione Finale ed Allegati, CNRGNDCI, http://avi.gndci.cnr.it/, Italy, 1998. Accessed Jan 4 2020

Bacilieri C (2019) I borghi più belli d'Italia 2019–2020. Il fascino dell'Italia nascosta, Società Editrice Romana

Barbano MS, Pappalardo G, Pirrotta C, Mineo S (2014) Landslide triggers along volcanic rock slopes in eastern Sicily (Italy). Natural Hazards 73 (3):1587-1607

Baroň I, Bečkovský D, Míča L (2014) Application of infrared thermography for mapping open fractures in deep-seated rockslides and unstable cliffs. Landslides 11 (1):15-27

Baroň I, Bečkovský D, Míča L (2012) Application of infrared thermography for mapping open fractures in deepseated rockslides and unstable cliffs. Landslides 11:15–27. https://doi.org/10.1007/s10346-012-0367-z

Bieniawski ZT (1989) Engineering rock mass classification. John Wiley& Son, New York 251 pp

Casagli N, Frodella W, Morelli S, Tofani V, Ciampalini A, Intrieri E, Raspini F, Rossi G, Tanteri L, Lu P (2017) Spaceborne, UAV and ground-based remote sensing techniques for landslide mapping, monitoring and early warning. Geoenviron Disasters 4:9

Castellaro S, Mulargia F (2009) The effect of velocity inversions on H/V. Pure Appl Geophys 166(4):567–592. https://doi.org/10.1007/s00024-009-0474-5

Danneels G, Bourdeau C, Torgoev I, Havenith HB (2008) Geophysical investigation and dynamic modelling of unstable slopes: case-study of Kainama (Kyrgyzstan). Geophys J Int 175(1):17–34

Del Gaudio V, Coccia S, Wasowski J, Gallipoli MR, Mucciarelli M (2008) Detection of directivity in seismic site response from microtremor spectral analysis. Nat Hazards Earth Syst Sci 8(4):751–762. https://doi.org/10.5194/nhess-8-751-2008

Del Gaudio V, Wasowski J, Muscillo S (2013) New developments in ambient noise analysis to characterise the seismic response of landslide-prone slopes. Nat Hazards Earth Syst Sci 13(8):2075–2087

Fanti R, Gigli G, Lombardi L, Tapete D, Canuti P (2012) Terrestrial laser scanning for rockfall stability analysis in the cultural heritage site of Pitigliano (Italy). Landslides 10:409–420

Ferrara V, Pappalardo G (2005) Kinematic analysis of rock falls in an urban area: the case of Castelmola hill near Taormina (Sicily, Italy). Geomorphology 66:373–383

FLIR (2015) User's manual FLIR tools/tools+. Publ n T559600, 152pp

Frodella W, Gigli G, Morelli S, Lombardi L, Casagli N (2017a) Landslide mapping and characterization through infrared thermography (IRT): suggestions for a methodological approach from some case studies. Remote Sens 2017(9):1281. https://doi.org/10.3390/rs9121281

Frodella W, Morelli S, Pazzi V (2017b) Infrared thermographic surveys for landslide mapping and characterization: the Rotolon Dsgsd (northern Italy) case study. Italian journal of engineering geology and environment, Special Issue 1(2017):77–84

Gigli G, Morelli S, Fornera S, Casagli N (2014a) Terrestrial laser scanner and geomechanical surveys for the rapid evaluation of rock fall susceptibility scenarios. Landslides 11:1–14. https://doi.org/10.1007/s10346-012-0374-0

Gigli G, Frodella W, Garfagnoli F, Morelli S, Mugnai F, Menna F, Casagli N (2014b) 3-D geomechanical rock mass characterization for the evaluation of rockslide susceptibility scenarios

Gross MR (1995) Fracture partitioning: failure mode as a function of lithology in the Monterey formation of coastal California. Geol Soc Am Bull 107(7):779–792

Hillel D (1998) Environmental soil physics. Academic Press, New York 771 pp

Ibs-von Seht M, Wohlenberg J (1999) Microtremor measurements used to map thickness of soft sediments. Bull Seism Soc Am 89(1):250–259

Imposa S, Coco G, Corrao M (2004) Site effects close to structural lineaments in eastern Sicily (Italy). Eng Geol 72(3):331–341

Imposa S, Corrao M, Barone F, Coco G, Occhipinti R, Mozzicato P (2010) Geostructural and geognostic survey for a stability analysis of the calcareous cliff of Ispica (Hyblean plateau, southeastern Sicily). Bull Eng Geol Environ 69(2):247–256

Imposa S, Mele G, Corrao M, Coco G (2015) Borehole seismic surveys for the mechanical characterization of a calcarenite cliff in the area of Ispica (southern Sicily). Bull Eng Geol Environ 74(3):971–980. https://doi.org/10.1007/s10064-014-0683-8

Imposa S, Grassi S, Fazio F, Rannisi G, Cino P (2017a) Geophysical surveys to study a landslide body (North-Eastern Sicily). Nat Hazards 86(2):327–343

Imposa S, Panzera F, Grassi S, Lombardo G, Catalano S, Romagnoli G, Tortorici G (2017b) Geophysical and geologic surveys of the areas struck by the August 26th 2016 Central Italy earthquake: the study case of Pretare and Piedilama. J Appl Geophys 145:17–27

Lachet C, Bard PY (1994) Numerical and theoretical investigations on the possibilities and limitation of Nakamura's technique. J Phys Earth 42(5):377–397. https://doi.org/10.4294/jpe1952.42.377

Lato MJ, Diederichs MS, Hutchinson DJ, Harrap R (2012) Evaluating roadside rockmasses for rockfall hazards using LiDAR data: optimizing data collection and processing protocols. Nat Hazards 60:831–864

Lermo J, Chavez-Garcia FJ (1993) Site effect evaluation using spectral ratios with only one station. Bull Seismol Soc Am 83:1574–1594

Lentini F, Carbone S, Guarnieri P (2006) Collisional and postcollisional tectonics of the Apenninic-Maghrebian orogen (southern Italy). In Geological Society of America Special Paper 409; Geological Society of America: Boulder, CO, USA, 2006; pp. 57–81.

Lim M, Petley DN, Rosser NU, Allison RJ, Long AJ, Pybus D (2005) Combined digital photogrammetry and time-of-flight laser scanning for monitoring cliff evolution. Photogramm Rec 20:109–129

Tortorici L, Monaco C, Tansi C, Cocina O (1985) Recent and active tectonics in the Calabrian arc (Southern Italy). Tectonophysics 243 (1-2):37-55

Martino S, Mazzanti P (2014) Integrating geomechanical surveys and remote sensing for sea cliff slope stability analysis: the Mt. Pucci case study (Italy). Nat Hazards Earth Syst Sci 14:831–848. https://doi.org/10.5194/nhess-14-831-2014
Marinos P, Tsiambaos G (2002) Earthquake Triggering Rockfalls Affecting Historic Monuments and a Traditional Settlement in Skyros Island, Greece. In International Symposium on Landslide Risk Mitigation and Protection of Cultural and Natural Heritage, 21-25 January 2002, Kyoto, Japan, 343-346
Meola C, Carlomagno GM (2004) Recent advances in the use of infrared thermography. Meas Sci Technol 15:27–58
Mineo S, Pappalardo G (2016a) The use of infrared thermography for porosity assessment of intact rock. Rock Mech Rock Eng 49(8):3027–3039. https://doi.org/10.1007/s00603-016-0992-2
Mineo S, Pappalardo G (2016b) Preliminary results on the estimation of porosity in intact rock through infrared thermography. Rend Online Soc Geol It 41:317–320. https://doi.org/10.3301/ROL.2016.157
Mineo S, Pappalardo G (2019) Infrared thermography presented as an innovative and non-destructive solution to quantify rock porosity in laboratory. Int J Rock Mech Min Sci 115:99–110. https://doi.org/10.1016/j.ijrmms.2019.01.012
Mineo S, Pappalardo G, Rapisarda F, Cubito A, Di Maria G (2015a) Integrated geostructural, seismic and infrared thermography surveys for the study of an unstable rock slope in the Peloritani chain (NE Sicily). Eng Geol 195:225–235. https://doi.org/10.1016/j.enggeo.2015.06.010
Mineo S, Calcaterra D, Perriello Zampelli S, Pappalardo G (2015b) Application of infrared thermography for the survey of intensely jointed rock slopes. Rend Online Soc Geol It 35:212–215. https://doi.org/10.3301/ROL.2015.103
Mineo S, Pappalardo G, D'Urso A, Calcaterra D (2017) Event tree analysis for rockfall risk assessment along a strategic mountainous transportation route. Environ Earth Sci 76(17):620–621. https://doi.org/10.1007/s12665-017-6958-1
Mineo S, Pappalardo G, Mangiameli M, Campolo S, Mussumeci G (2018) Rockfall analysis for preliminary hazard assessment of the cliff of Taormina Saracen Castle (Sicily). Sustainability 10(2):417. https://doi.org/10.3390/su10020417
Monsalve JJ, Baggett J, Bishop R, Ripepi N (2019) Application of laser scanning for rock mass characterization and discrete fracture network generation in an underground limestone mine. Int J Min Sci Technol 29:131–137
Nakamura Y (1989) A method for dynamic characteristics estimation of subsurface using microtremor on the ground surface. Railw Tech Res Inst Q Rep 30:25–33
Niu J, Oyediran IA, Liu D, Huang X, Cui Z, Wang H, Shi X (2015) Quantitative foundation stability evaluation of urban karst area: Case study of Tangshan, China. Soils Found 55(3):493–503
Nogoshi M, Igarashi T (1970) On the propagation characteristics of the microtremors. J Seismol Soc Jpn 24:24–40
Okada H (2003) The microtremor survey method. Geophys Monogr Ser Soc Explor Geophys 12:150
P.A.I.: Piano Stralcio di Bacino per l'Assetto Idrogeologico, Regione Siciliana, http://www.sitr.regione.sicilia.it/pai/ (2006) accessed 2019
Pappalardo G (2015) Correlation between P-wave velocity and physical-mechanical properties of intensely jointed dolostones, Peloritani mounts, NE Sicily. Rock Mech Rock Eng 48:1711–1721. https://doi.org/10.1007/s00603-014-0607-8
Pappalardo G (2018) First results of infrared thermography applied to the evaluation of hydraulic conductivity in rock masses. Hydrogeol J 1–12
Pappalardo G, Mineo S (2015) Rockfall hazard and risk assessment: the promontory of the pre-Hellenic Village Castelmola Case, North-Eastern Sicily (Italy). In: Lollino G et al (eds) Engineering Geology Society Territory—Volume 2, 1989–1993. https://doi.org/10.1007/978-3-319-09057-3_353
Pappalardo G, Mineo S (2016) Microstructural controls on physical and mechanical properties of dolomite rocks. Rend Online Soc Geol It 41:321–324. https://doi.org/10.3301/ROL.2016.158
Pappalardo G, Mineo S (2017) Investigation on the mechanical attitude of basaltic rocks from Mount Etna through infrared thermography and laboratory tests. Constr Build Mater 134:228–235. https://doi.org/10.1016/j.conbuildmat.2016.12.146
Pappalardo G, Mineo S (2019) Study of jointed and weathered rock slopes through the innovative approach of InfraRed thermography. In: Pradhan S, Vishal V, Singh T (eds) Landslides: theory, practice and Modelling. Advances in natural and technological hazards research, vol 50. Springer, Cham. https://doi.org/10.1007/978-3-319-77377-3_5
Pappalardo G, Mineo S, Rapisarda F (2014) Rockfall hazard assessment along a road on the Peloritani Mountains (northeastern Sicily, Italy). Nat Hazards Earth Syst Sci 14:2735–2748. https://doi.org/10.5194/nhess-14-2735-2014
Pappalardo G, Mineo S, Perriello Zampelli S, Cubito A, Calcaterra D (2016a) InfraRed thermography proposed for the estimation of the cooling rate index in the remote survey of rock masses. Int J Rock Mech Min Sci 83:182–196. https://doi.org/10.1016/j.ijrmms.2016.01.010
Pappalardo G, Imposa S, Mineo S, Grassi S (2016b) Evaluation of the stability of a rock cliff by means of geophysical and geomechanical surveys in a cultural heritage site (south-eastern Sicily). Ital J Geosci 135(3):1–47
Pappalardo G, Mineo S, Calcaterra D (2017) Geomechanical analysis of unstable rock wedges by means of geostructural and infrared thermography surveys. Ital J Eng Geol Environ Spec Issue (2017):93–101. https://doi.org/10.4408/IJEGE.2017-01.S-09
Pappalardo G, Mineo S, Angrisani AC, Di Martire D, Calcaterra D (2018a) Combining field data with infrared thermography and DInSAR surveys to evaluate the activity of landslides: the case study of Randazzo landslide (NE Sicily). Landslides 15:2173–2193. https://doi.org/10.1007/s10346-018-1026-9
Pappalardo G, Imposa S, Barbano MS, Grassi S, Mineo S (2018b) Study of landslides at the archaeological site of Abakainon necropolis (NE Sicily) by geomorphological and geophysical investigations. Landslides 15:1279–1297. https://doi.org/10.1007/s10346-018-0951-y
Park CB, Miller RD, Xia J (1999) Multichannel analysis of surface waves. Geophysics 64(3):800–808
Pratesi F, Nolesini T, Bianchini S, Leva D, Lombardi L, Fanti R, Casagli N (2014) Integrated TLS and GBInSAR system for monitoring structural instabilities over urbanized areas: the case of Volterra (Tuscany, Italy). Conference: 139. DVW-seminar Terrestrisches Laserscanning 2014 (TLS 2014), at Fulda
Rees WG (2001) Physical principles of remote sensing. Cambridge University Press, p 343
Rosser NU, Petley DN, Lim M, Dunning SA, Allison RJ (2005) Terrestrial laser scanning for monitoring the process of hard rock coastal cliff erosion. Q J Eng Geol Hydrogeol 38:363–375
Santo A, Del Prete S, Di Crescenzo G, Rotella M (2007) Karst processes and slope instability: some investigations in the carbonate Apennine of Campania (southern Italy). In: Parise M, Gunn J (eds) Natural and anthropogenic hazards in karst areas: recognition, analysis and mitigation. Geological society, London, special publications, 279, 59–72. https://doi.org/10.1144/SP279.60305-8719/07/$15.00. The Geological Society of London
Saroglou H, Marinos V, Marinos P, Tsiambaos G (2012) Rockfall hazard and risk assessment: an example from a high promontory at the historical site of Monemvasia. Greece, Nat Hazards Earth Syst Sci 12:1823–1836. https://doi.org/10.5194/nhess-12-1823-2012
Shannon HR, Sigda JM, Van Dam RL, Handrickx JMH, McLemore VT (2005) Thermal camera imaging of rock piles at the Questa Molybdenum Mine, Questa, New Mexico. Proc. 2005 National Meeting of the American Society of Mining and Reclamation, June 19–23, ASMR: 1015–1028
Squarzoni C, Galgaro A, Teza G, Acosta CAT, Pernito MA, Bucceri N (2008) Terrestrial laser scanner and infrared thermography in rock fall prone slope analysis. Geophysical Research Abstracts, Vol. 10, EGU2008-A-09254
Teza G, Marcato G, Castelli E, Galgaro A (2012) IRTROCK: a MATLAB toolbox for contactless recognition of surface and shallow weakness of a rock cliff by infrared thermography. Comput Geosci 45:109–118
Teza G, Marcato G, Pasuto A, Galgaro A (2015) Integration of laser scanning and thermal imaging in monitoring optimization and assessment of rockfall hazard: a case history in the Carnic Alps (Northeastern Italy). Nat Hazards 76:1535–1549. https://doi.org/10.1007/s11069-014-1545-1
Walsh SJ, Page PH, Brewington L, Bradley JR, Mena CF (2018) A beach vulnerability frameworl for the Galapagos Islands: fusion of Worldview-2 imagery, 3-D laser scanner data, and unmanned aerial vehicles. Compr Remote Sens 9:159–176
Wu JH, Lin HM, Lee DH, Fang SC (2005) Integrity assessment of rock mass behind the shotcreted slope using thermography. Eng Geol 80:164–173

G. Pappalardo · S. Mineo (✉) · S. Imposa · S. Grassi · D. Salerno
Department of Biological, Geological and Environmental Sciences,
University of Catania,
Corso Italia 57, Catania, Italy
Email: smineo@unict.it

A. Leotta · F. La Rosa
Geoverticale S.r.l,
Via Tezzano 35, Catania, Italy